EFFECT OF CHROMIUM DOPANT TOWARDS THE PHYSICAL AND CHEMICAL PROPERTIES OF VANADIUM PHOSPHORUS OXIDE CATALYSTS

JASLYN LOO SHEN - WUI

UNIVERSITI TUNKU ABDUL RAHMAN

EFFECT OF CHROMIUM DOPANT TOWARDS THE PHYSICAL AND CHEMICAL PROPERTIES OF VANADIUM PHOSPHORUS OXIDE CATALYSTS

JASLYN LOO SHEN - WUI

A project report submitted in partial fulfilment of the requirements for the award of the degree of Bachelor of Engineering (Hons) Chemical Engineering

Faculty of Engineering and Science
Universiti Tunku Abdul Rahman

May 2011

DECLARATION

I hereby declare that this project report is based on my original work except for citations and quotations which have been duly acknowledged. I also declare that it has not been previously and concurrently submitted for any other degree or award at UTAR or other institutions.

Signature : _____

Name : ____Jaslyn Loo Shen- Wui___

ID No. : _____07UEB02944_____

Date : _____10th May 2011_____

APPROVAL FOR SUBMISSION

I certify that this project report entitled **"EFFECT OF CHROMIUM DOPANT TOWARDS THE PHYSICAL AND CHEMICAL PROPERTIES OF VANADIUM PHOSPHORUS OXIDE CATALYSTS"** was prepared by **JASLYN LOO SHEN-WUI** has met the required standard for submission in partial fulfilment of the requirements for the award of Bachelor of Engineering (Hons.) Chemical Engineering at Universiti Tunku Abdul Rahman.

Approved by,

Signature : _____

Supervisor : Dr. Leong Loong Koong

Date : _____

Specially dedicated to
my beloved father and mother.
God loves them both.

ACKNOWLEDGEMENTS

I would like to thank everyone who had contributed to the successful completion of this project. I would like to express my gratitude to my research supervisor, Dr. Leong Loong Koong for his invaluable advice, guidance and patience throughout the development of the research.

In addition, I would also like to express my sincere gratitude to the fellow Master students of Dr. Leong: Max, Katherine, and Zoey for their constant supervision. They have dedicated their time, relentlessly helping me out and guiding me throughout the research until completion.

Last but not least, many thanks to my fellow coursemates who are also under Dr. Leong's supervision: Johnathan Har, Jonathan Ow, Hii Shin Yi, Wong Pei Wen, Tan Ling Han and Chen Jian Jie for being around to provide needful assistance throughout the experiment.

EFFECT OF CHROMIUM DOPANT TOWARDS THE PHYSICAL AND CHEMICAL PROPERTIES OF VANADIUM PHOSPHORUS OXIDE CATALYSTS

ABSTRACT

0.1 wt%, 0.3 wt% and 0.5 wt% chromium-promoted VPO catalysts and unpromoted vanadyl pyrophosphate, VPO catalysts were synthesized via $VOHPO_4 \cdot 1.5H_2O$ precursor synthesis route. The samples were calcined in 0.75 % *n*-butane/air environment at 460℃ for 24 hours and were denoted as BulkVPO, 0.1CrVPO, 0.3CrVPO and 0.5CrVPO. The physical and chemical properties were studied by XRD, BET, SEM-EDAX, redox titration and ICP-OES. Results from XRD analysis had found that the crystallite size of plane (2 0 4) had decreased from 111.3192 Å to 95.5499 Å. The specific surface area measured from BET analysis had shown increment from 8.76 m^2 g^{-1} to 27.32 m^2 g^{-1} as well with increasing promoter concentration. This corresponds to the XRD results that having decreasing crystallite size will mean having bigger specific surface area. Observation from SEM showed that all samples displayed plate-like crystals formed in rosette agglomerates. EDX study had detected the presence of vanadium and phosphorus in all VPO samples. The presence of chromium in increasing amount was detected in only the promoted samples. The average valence from redox titration was found to be ranging from 4.2326 to 4.7021. The average P/V obtained from ICP-OES was 1.28.

TABLE OF CONTENTS

LIST OF TABLES

LIST OF FIGURES

LIST OF SYMBOLS / ABBREVIATIONS

T	Crystallite size, Å
λ	Wavelength, Å
$VOHPO_4 \cdot 0.5H_2O$	Vanadyl Hydrogen Phosphate Hemihydrate
$VOHPO_4 \cdot 1.5H_2O$	Vanadyl Hydrogen Phosphate Sesquihydrate
$VOPO_4 \cdot 2H_2O$	Vanadyl Phosphate Dihydrate
VPO	Vanadyl pyrophosphate, $(VO)_2P_2O_7$
BET	Brunauer, Emmett and Teller
SEM	Scanning Electron Microscope
EDX	Energy-Dispersive X-ray Spectroscopy
FWHM	Full-Width at Half-Maximum
P/V	Phosphorus to vanadium ratio
CrVPO	Chromium promoted VPO catalyst

LIST OF APPENDICES

CHAPTER 1

INTRODUCTION

1.1 Catalysis and Catalyst

Catalysis is defined as the occurrence, study and use of catalysts and catalytic processes (Fogler, 2006). In industrial processes, catalysts are used to accelerate a chemical reaction. A catalyst is a substance that affects the rate of a reaction but emerges from the process unchanged. A catalyst usually changes a reaction rate by promoting a different molecular path or mechanism for the reaction. It does so by forming bonds with the reacting molecules, and by allowing these to react to a product, which detaches from the catalyst, and leaves it unaltered such that it is available for the next reaction (Chorkendorff and Niemantsverdriet, 2003).

Catalysts have been used by humans for over 2000 years (Oyama and Somorjai, 1986), with major uses being in upstream and downstream petroleum refining, petrochemical production, food processing like wine, cheese and bread etc. A catalyst makes it possible to obtain an end product by a different pathway with a lower energy barrier. For this, it can affect both the yield and selectivity.

Catalysts will lower the original activation energy of the chemical reaction, facilitating the reaction to occur when reactants form chemisorptions bonds with the catalyst surface. The reactants will overcome the potential barrier with lower activation energy to form desired product. While the catalyst lowers the activation energy, it does not change the energies of the original reactants nor products. An energy profile of a typical behaviour of catalysts is illustrated in Figure 1.1.

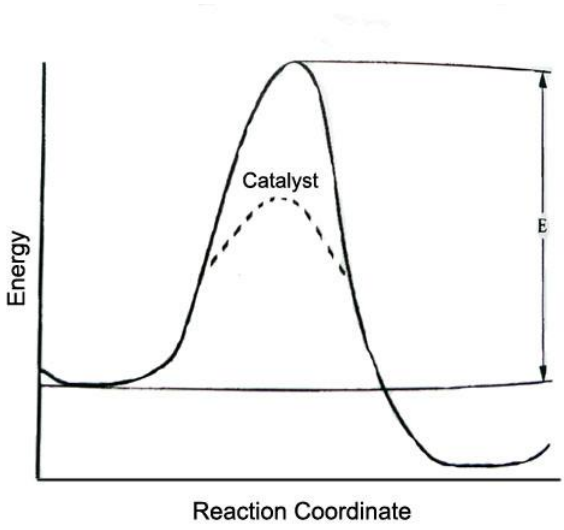

Figure 1.1: Presence of Catalyst in The Activation Energy Profile

1.2 Types of Catalysts

There are two types of catalysts in the market, namely the homogeneous catalyst and the heterogeneous catalyst. To define, homogeneous catalyst is a catalyst that is in solution with at least one of the reactants. In homogeneous catalysis, both the catalyst and the reactants are in the same phase. All molecules are either in the gas phase or liquid phase. An example of homogeneous catalysis is the industrial oxo process of isobutylaldehyde with cobalt complex as the catalyst (Fogler, 2006).

On the other hand, heterogeneous catalyst is a catalyst that involves more than one phase. Usually, the catalyst is a solid and the reactants and products are in liquid or gaseous form. Catalytic reactions for solid catalyst usually occur at the surface itself. Heterogeneous catalyst is more common as it is simple to separate from the product. As such, it is more economically attractive, especially when catalyst itself is quite valuable and needs to be constantly reused. An example of heterogeneous catalyst used is platinum-on-alumina during dehydrogenation of cyclohexane to produce benzene (Fogler, 2006).

1.3 Essential Properties of Good Catalysts

It is important to determine the vital properties of catalysts as such they can be utilised more economically. Catalysts usually exist in fine particles, are porous, can withstand extreme condition and can be pelletized for industrial application purposes. General good properties of catalysts are further described below.

Catalyst should contain large surface area as it is important to obtain significantly optimum reaction rate. Generally, this area is provided by an inner porous structure i.e. containing many fine pores. The surface of these pores supplies the area needed for high rate of reaction (Fogler, 2006).

In addition to that, good catalysts should act like molecular sieves. The structure of the pores is one of the reasons behind the selectivity of the catalyst. The pores behave in such a way that they will admit small molecules but prevent large ones from entering. Besides controlling the residence time of the reactant near the catalytically active surface, it can also configure the reactants in such a way that only a certain orientation can react. An example of such catalyst is zeolite catalysing the formation of para-xylene from toluene and methane (Fogler, 2006).

In addition, good catalysts should be stable to withstand mechanical shear and other extreme conditions. They are able to be formed into required shapes as such they do not cause pressure drop and unnecessary hot spots in a reactor. A typical example for such a characteristic is the platinum gauze reactor used in ammonia oxidation of nitric acid as platinum is the primary material in the monolith (Fogler, 2006).

Last but not least, good catalysts are able to maintain their activities at the same levels for longer periods before experiencing deactivation by aging, poisoning, coking or fouling etc. They should be subjected to the ease of reactivation. (Fogler, 2006)

1.4 Importance and Uses of Catalysts

Often chemical reactions can be controlled by manipulating the temperature, concentration, pressure and residence time. Although raising the temperature and pressure will enable stoichiometric reactions to proceed at a reasonable rate of production, safety and financial feasibility may become problematic issues. Without catalysts, many chemical reactions will not be possible to carry out as non-catalytic, stoichiometric reactions are generally not economical.

Generally, catalysts accelerate reactions by orders of magnitude, enabling them to be carried out under favourable conditions. With efficient catalysts together with optimized reactor and total plant design, reactions become more favourable and feasible. In addition to that, catalytic routes are part of applications for green technology. This is because catalysts use raw materials efficiently, the formation of waste or undesirable by-products can be minimized substantially (Chorkendorff and Niemantsverdriet, 2003).

In fact, short term, evolutionary approaches focusing on the improvement of current catalytic technologies and processes are underway. Researches for substitution of hazardous chemicals and solvents which can revamp plants and environmental cleanup technologies with catalysts are continuously conducted to make sure that all emissions meet legislative regulations as well as to help preserve a better environment. (Centi and Perathoner, 2003)

1.5 Problem Statement

To date, the optimum selectivity and activity for VPO catalyst in the production of maleic anhydride, MA are still in extensive studies. Based on the production information from BASF Petronas (2010), the maximum conversion (activity) of VPO catalyst attempted was at 82 % with 65 % selectivity. It is yet to determine the potential of low-doped chromium in improving the catalytic performance of VPO catalyst to produce MA.

As such, this research will study the effect of various concentrations of low-doped chromium dopant (0.1 wt%, 0.3 wt% and 0.5 wt%) used to promote the existing VPO catalyst in the hope to increase the its selectivity.

1.6 Objective of Research

1. To synthesise vanadyl pyrophosphate, VPO via sesquihydrate precursor route.
2. To study the effect of various chromium concentrations towards the physical and chemical properties of chromium-doped VPO catalysts.

CHAPTER 2

LITERATURE REVIEW

2.1 Maleic Anhydride, MA

Maleic Anhydride is versatile and widely used in the manufacturing of chemical products, typically in polycondensation of engineering plastics and miscellaneous addition reactions. It is prevalent as chemical intermediates in the chemical industry, especially as the co-monomer in the syntheses of unsaturated polyester resins (UPR) (Hutchings G. J., 1990). MA is also used in the production of alkyd resins, lacquers, plasticizers, copolymers and lubricants (Moulijn *et al.*, 1993). They are also used as part of the agricultural chemicals, dye intermediates, and pharmaceuticals products. MA is also ingredient in bonding agents used to manufacture plywood, a corrosion inhibitor, and a preservative in oils and fats.

The application of maleic anhydride and maleic anhydride copolymers has driven recyclability, biodegradability and the use of more sustainable chemicals to a greater level. Many organizations have directed their companies' policies to environmental conversation. As such, much attention has been given to renewable sources or replacing one petroleum-based chemicals with more environmentally friendly products. As of present, approximately 51 % of global MA product was used for the production of UPR and the statistics is still increasing.

2.2 Oxidation of *n*-Butane to MA

The oxidation of *n*-butane is carried out in fixed-bed, fluid-bed or circulating fluid-bed riser reactors. In the past, MA is produced by the partial oxidation of benzene. However, the most recent production of MA is via the oxidation of n-butane. The production MA with the raw material of *n*-butane has largely replaced the original starting material, benzene. This is because benzene is carcinogenic, hazardous and toxic to living beings if released to the environment. The chemical reaction of oxidation of *n*-butane to MA is given as below (Moulijn *et al.*, 1993):

$$C_4H_{10} + 3.5O_2 \xrightarrow[VPO]{} C_4H_2O_3 + 4H_2O \qquad \Delta H = -1260 \text{ kJ/mol}$$

The selective oxidation of *n*-butane to maleic anhydride is largely catalysed by vanadyl pyrophosphate, VPO to increase the yield of MA. However, there are another three types of catalysts for alkane oxidation, namely Magnesium orthovanadate, $Mg_3(VO_4)_2$, Magnesium pyrovanadate, $Mg_2V_2O_7$ and VPO, $(VO)_2P_2O_7$. VPO is chosen as it contains the highest conversion from n-butane to MA. As such, extensive studies and researches to obtain the best properties of VPO have been continuously conducted to develop the best form of VPO to boost MA's productivity.

2.3 Vanadyl Pyrophosphate Catalyst (VPO), $(VO)_2P_2O_7$

Vanadyl pyrophosphate (VPO), $(VO)_2P_2O_7$ is the catalyst most commonly used in the production of maleic anhydride. As vanadium exists in several oxidation numbers i.e. +5, +4 and +3, there are different VPO phases formed, with each of these phases contributing to different morphology and properties in the catalytic system (Abon and Volta, 1997).

The V^{5+} phase comprises hydrates like $VOPO_4 \cdot H_2O$, $VOPO_4 \cdot 2H_2O$ and phosphates $VOPO_4$. The V^{4+} phase is of hydrogenophosphates like $VOPO_4 \cdot 0.5H_2O$, $VOHPO_4.4H_2O$ or $VO(H_2PO_4)_2$ to pyrophosphate $(VO)_2P_2O_7$ to metaphosphates $VO(PO_3)_2$; whilst the V^{3+} phase consists of VPO_4 and $V(PO_3)_3$. The V^{5+} vanadyl hydrates and hydrogenophosphates in V^{4+} are generally considered as the catalysts precursors. In VPO catalytic system, the most important phases are V^{4+} and V^{5+} which corresponds to the activity and selectivity of the catalyst respectively.

2.4 Preparation of VPO Catalyst

There are notably a few types of syntheses for VPO catalyst, for instance aqueous medium, organic medium, vandyl phosphate dihydrate precursor, vanadyl phosphate hemihydrate precursor, vanadyl phosphate sesquihydrate precursor and ball milling. Each of these methods produces different types of precursors with different morphology, chemical and physical properties. Individual synthesis route is explained in subsequent subsections respectively.

Generally, there are two types of mediums that can be used in the preparative route for reduction process. They are the aqueous and organic medium. Each of them contributes to different morphological structure of the resulting VPO catalysts. Preparation in aqueous medium involves vanadium pentoxide, V_2O_5 being reduced by mineral agents i.e. HCl, N_2H_4 etc. in water before adding ortho-phosphoric acid. As for organic medium, V_2O_5 is reduced by organic reagents like methanol, tetrahydrofuran or isobutanol before adding ortho-phosphoric acid into the mixture (Abon and Volta, 1997).

2.4.1 Dihydrate Precursor Synthesis

For dihydrate synthesis, $VOPO_4 \cdot 2H_2O$ material was prepared by reacting V_2O_5 with ortho−phosphoric acid, *o*−H_3PO_4 in water under reflux with continuous stirring for 24 hours (Taufiq-Yap *et al.*, 2008). The yellow solid was then recovered by filtration, washed with distilled water and followed by acetone. It was dried at 383 K for overnight. After that, the synthesized $VOPO_4 \cdot 2H_2O$ was suspended by rapid stirring into isobutyl alcohol and the mixture was refluxed for 21 hours with continuous stirring. A blue solid was recovered by filtration and washed with distilled water followed by acetone. The resulting blue solid, $VOHPO_4 \cdot 0.5H_2O$ was further treated in refluxing water for 3 hours to remove $VO(H_2PO_4)_2$ and was separated by filtration and dried overnight in air at 385 K (Hutchings *et al.*, 2003).

2.4.2 Hemihydrate Precursor Synthesis

The vanadyl phosphate hemihydrate precursors were prepared via organic route by the reaction of V_2O_5 with isobutanol in the solvent of benzyl alcohol. The reaction mixture was refluxed for 7 h at 393 K, the mixture was cooled to room temperature and was left stirring overnight. Then ortho-phosphoric acid, *o*-H3PO4 was added to obtain the desired P/V atomic ratio of 1.0. The mixture was further refluxed for another 3 hours at 393 K with stirring. The obtained blue slurry was cooled to room temperature and the solid was recovered by a centrifuge. The solid was washed sparingly with water and dried in air at 373 K for 24 hours. $VOHPO_4 \cdot 0.5H_2O$ was activated in a reaction flow of *n*-butane in air mixture (0.75% *n*-butane in air) at 673 K for 6 hours. (Taufiq-Yap, 2006)

2.4.3 Sesquihydrate Precursor Synthesis

Sesquihydrate precursor was obtained by reacting V_2O_5 with $o-H_3PO_4$ in water under reflux with continuous stirring for 24 hours to obtain yellow slurry. The solid intermediate was recovered with centrifugation and left to dry to obtain yellow powder, which was vanadium phosphate dihydrate, $VOPO_4 \cdot 2H_2O$ (Ishimura *et al.*, 2000). $VOPO_4 \cdot 2H_2O$ was then further reduced by 1-butanol for 24 hours. The precursor is then activated by calcination and revealed high specific activity in vapour-phase oxidation of *n*-butane. (Taufiq-Yap *et al.*, 2004)

2.5 Parameters of VPO Catalyst

The catalytic performance depends strongly on the characteristics of the vanadium phosphorus oxides catalyst derived from the preparation of the vanadyl hydrogen phosphate precursor. Research on the VPO system has been largely developed in the last decade. Many publications of journals have been devoted to this formulation and the study is still on-going.

Many experimental parameters have been examined specifically on the nature of the reducing agent or solvents, the effect of promoters and support system, the P/V ratio, and the calcination conditions (Abon and Volta, 1997). All these parameters are believed to influence the final phase of the catalysts and the distribution of phosphorus vanadium (P/V) and its oxidation state. The parameters involved are discussed in subsections 2.5.1 – 2.5.4.

2.5.1 Calcination Condition

The transformation of precursor to the active phase of VPO catalyst is done by calcining the precursor. In laboratory scale, calcination is done in a tubular furnace with the powdered precursor being flown with a mixture of calcination agents, commonly *n*-butane in air for a specific period of time. The surface chemistry and bulk properties of VPO can be affected by various calcination environments, namely temperature, duration and different types of calcination agents which will affect the crystalline phases of the catalyst structure. Different condition will ultimately affect the different phases portrayed on the catalytic performances in selective oxidation of *n*-butane.

Numerous past studies suggested that a combination of vanadyl pyrophosphate along with patches of $VOPO_4$ phases play an important role in the selective oxidation of *n*-butane. However, little studies concerning the VPO active sites on other calcination agents, notably on the selective oxidation of propane have been done. To study this parameter, Yap and Saw used two types of calcination agent i.e. n-butane/air and propane/air for the calcination process (Taufiq-Yap and Saw, 2008).

From the catalytic test, they found that *n*-butane calcined catalyst show higher conversion for both hydrocarbons oxidation compared to the propane/air calcined catalyst. This is due to the behaviour of active oxygen atom, O^- in the catalysts playing a vital role in the activation of *n*-butane and propane. The authors had confirmed that this was the main determining step for the oxidation of hydrocarbons (Taufiq-Yap and Saw, 2008). As such, *n*-butane was concluded widely used for the partial oxidation process to maleic anhydride, MA.

2.5.2 Support System

A support is an inactive substance enabling the active substance, in this case, the catalyst to mount onto it for support. Supported VPO express superior characteristics over the bulk VPO because it offers higher amount of active sites per unit mass catalyst and higher mechanical strength to withstand the extreme condition in the bed reactors.

However, it is reported that supported VPO catalysts usually consisted of V^{5+} species, mostly in α-$VOPO_4$ and/or γ-$VOPO_4$ form and exhibited low MA selectivity as well as low butane conversion. For instance, the silica-supported VPO catalyst had improved the MA selectivity. Unfortunately, only a slight increase in MA yield was achieved. (Ji *et al.*, 2003)

It is further explained that this was because the introduction of a support system could hinder the formation of the active $(VO)_2P_2O_7$ phase. Therefore, the resulted catalysts generally exhibited low butane conversion and poor MA selectivity. When there was a strong interaction between VPO and a reducible support i.e. titania or zirconia, the VPO became more reducible and the catalytic activity was remarkably higher. Despite so, with the application of a support such as silica, interaction with the active phase became less strongly. This had improved the selectivity but would decrease the conversion on the other hand. (Au *et al.*, 2004)

The experimental results from Do and Baerns confirmed that the catalytic performance of V_2O_5/P_2O_5 catalysts was dependent on the types of support used. They found that V_2O_5/P_2O_5 catalysts with TiO_2 exhibit a higher MA selectivity for the oxidation of but-1-ene and furan as compared to V_2O_5/P_2O_5 catalysts with Al_2O_3. On the other hand, Al_2O_3-supported catalyst showed greater activity than the TiO_2-supported catalyst for the non-selective consecutive oxidation of MA. There is a notably strong interaction between the support surface and the intermediates of the but-1-ene and furan oxidation leading to MA. Moreover, MA itself will interact with the surface as well. In summary, an optimized concentration between selectivity and activity of VPO catalyst in the support system is crucial to obtain the best yield of MA in the production (Baerns and Do, 1988).

2.5.3 Dopant

In industrial processes, many promoters have been studied aiming to improve the activity of VPO catalyst. Much attention and devotion have been paid to study different types of promoters in the hope to find the most suitable additive to enhance the performance of VPO in terms of selectivity and reactivity. The Lewis sites strength may be affected by the promoter as well.

Previous study on chromium doped VPO catalyst revealed that the addition of Cr yields catalysts with *ca.* 50% higher surface area than the unpromoted VPO. The presence of chromium may also affect the acidity of the base VPO. However, the authors found out that there was no correlation between surface area and Cr load. (Lombardo and Pierini, 2005)

In this research, the author has chosen chromium as the dopant of interest to be incorporated with the bulk VPO catalyst. It is believed that dopant intercalated in the structure of the VPO crystalline phase could increase the surface area of the VPO catalyst as well as its selectivity towards maleic anhydride production and reactivity.

2.5.4 P/V Atomic Ratio

The preparation route of VPO catalysts is most likely determined from the P/V (ratio of phosphorus to vanadium) ratio of the catalysts. It was found from a journal discussion that a correlation was observed between the onset of the oxidation of vanadium in dried catalysts upon calcination and the value of the surface P/V ratio.

According to the last researcher, the specific conversion increases by an order of magnitude for a P/V ratio exceeding unity. A slight excess of phosphorus with respect to 1:1 will result in the delay of in oxidation rate of vanadium. In fact, a P/V ratio of slightly higher than 1.0 corresponds to having a mean oxidation state of vanadium slightly higher than 4.0, which is the desired oxidation state to obtain the best activity and selectivity of the VPO catalysts (Garbassi *et al.*, 1986).

CHAPTER 3

METHODOLOGY

3.1 Materials and Gases Used

A list of chemicals and gases used throughout this study was as below:

1. Vanadium (V) pentoxide, V_2O_5 (MERCK)
2. ortho-phosphoric acid, *o*-H_3PO_4 (85 %) (MERCK)
3. 1-butanol, $CH_3(CH_2)_3OH$ (RandM Chemicals)
4. Nitric acid, HNO_3 (RandM Chemicals)
5. Sulphuric acid, H_2SO_4 (95 % − 98 %) (Systerm)
6. Chromium (III) nitrate nonahydrate, $Cr(NO_3)_3 \cdot 9H_2O$ (MERCK)
7. 0.75 % *n*-butane in air (Malaysia Oxygen Berhad, MOX)
8. 99.99 % purified nitrogen (Malaysia Oxygen Berhad, MOX)
9. 99.99 % purified helium (Malaysia Oxygen Berhad, MOX)
10. Liquid Nitrogen, N_2 (Malaysia Oxygen Berhad, MOX)
11. Diphenylamine, Ph_2NH indicator
12. 0.002 M Potassium permanganate, $KMnO_4$
13. 2 M sulphuric acid, H_2SO_4
14. 0.1 M sulphuric acid, H_2SO_4
15. 0.01 M ammonium iron(II)sulphate, $(NH_4)_2Fe(SO_4) \cdot 6H_2O$

3.2 Methodology

In this study, bulk VPO catalyst was prepared via vanadyl hydrogen phosphate sesquihydrate, $VOHPO_4 \cdot 1.5H_2O$ precursor route.

The synthesis procedure was done in two stages. The first stage began by obtaining vanadyl phosphate dihydrate, $VOPO_4 \cdot 2H_2O$ as an intermediate product from vanadium pentoxide, V_2O_5. In the second stage, $VOPO_4 \cdot 2H_2O$ was further reacted with 1-butanol to form the sesquihydrate, $VOHPO_4 \cdot 1.5H_2O$ precursor. A dopant of different concentration was added during this stage for promoted catalyst studies before the calcination process and would be discussed in subsections 3.2.1−3.2.2.

3.2.1 Preparation of Undoped VPO catalysts

15 g of vanadium pentoxide, V_2O_5 was added with 90 ml ortho-phosphoric acid, *o*-H_3PO_4 and 360 ml of water. The mixture was then refluxed for 24 hours at 120℃. A yellow intermediate, vanadyl phosphate dihydrate, $VOPO_4 \cdot 2H_2O$ was formed. Next, the sample was cooled down to room temperature before centrifuging it at 3000 rpm for 5 minutes. After that, the solid phase containing $VOPO_4 \cdot 2H_2O$ was recovered in an evaporating dish and left to dry in an oven at 85℃ for at least 24 hours. Lastly, $VOPO_4 \cdot 2H_2O$ was pounded into powder form and was therefore ready for the next stage. The apparatus setup for $VOPO_4 \cdot 2H_2O$ synthesis is shown in Figure 3.1.

Next, 10 g of $VOPO_4 \cdot 2H_2O$ bulk intermediate was added with 150 ml 1-butanol. The mixture was then refluxed for 24 hours at 120℃. Whitish-blue solution was formed during the reflux process (Figure 3.2). After that, the mixture was cooled down to room temperature before centrifuging it at 3000 rpm for 5 minutes. Next, the solid phase containing Cr-doped vanadyl hydrogen phosphate sesquihydrate, $VOHPO_4 \cdot 1.5H_2O$ was recovered in an evaporating dish and left to dry in an oven at 85℃ for at least 24 hours.

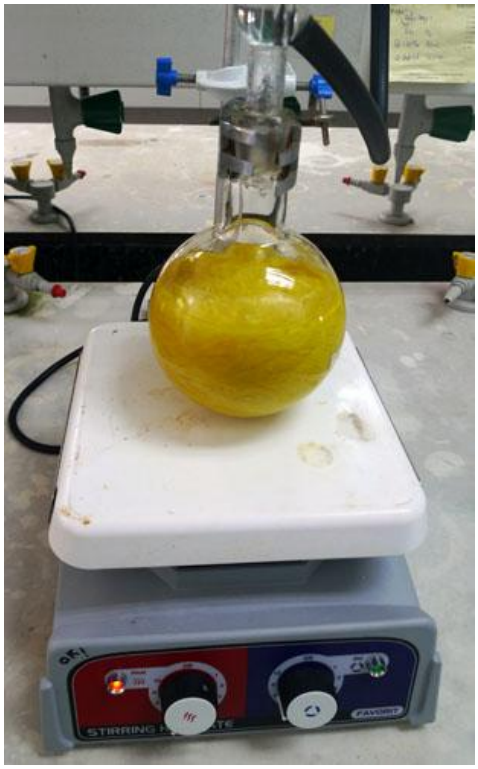

Figure 3.1 : Reflux process of vanadyl phosphate dihydrate, $VOPO_4 \cdot 2H_2O$

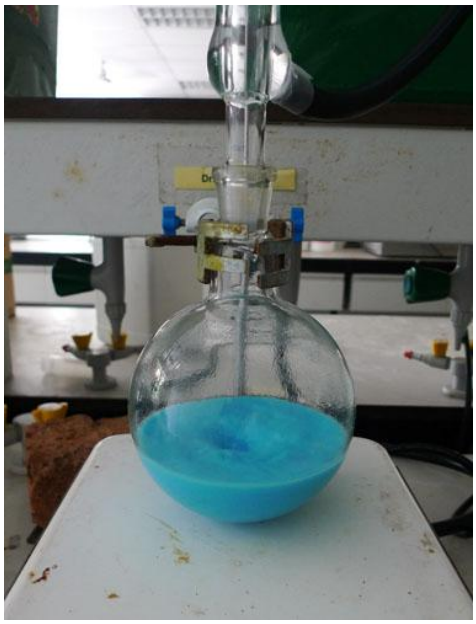

Figure 3.2 : Second reflux to obtain the sesquihydrate precursor, $VOHPO_4 \cdot 1.5H_2O$.

3.2.2 Preparation of Cr-doped VPO Catalysts

The preparation of Cr-doped precursor was exactly the same on the first stage. 15 g of vanadium pentoxide, V_2O_5 was added with 90 ml ortho-phosphoric acid, *o*-H_3PO_4 and 360 ml of water. The mixture was then refluxed for 24 hours at 120℃. A yellow intermediate, vanadyl phosphate dihydrate, $VOPO_4{\cdot}2H_2O$ was formed. Next, the sample was cooled down to room temperature before centrifuging it at 3000 rpm for 5 minutes. After that, the solid phase containing $VOPO_4{\cdot}2H_2O$ was recovered in an evaporating dish and left to dry in an oven at 85℃ for at least 24 hours. Lastly, $VOPO_4{\cdot}2H_2O$ was pounded into powder form and was therefore ready for the next stage. The apparatus setup for $VOPO_4{\cdot}2H_2O$ synthesis is shown in Figure 3.1.

Next, 10 g of $VOPO_4{\cdot}2H_2O$ bulk intermediate was added with 150 ml 1-butanol and 0.1 mol % (0.0202 g) of chromium(III)nitrate nonahydrate, $Cr(NO_3)_3{\cdot}\ 9H_2O$. The mixture was then refluxed for 24 hours at 120℃. Whitish-blue solution was formed during the reflux process (Figure 3.2). After that, the mixture was cooled down to room temperature before centrifuging it at 3000 rpm for 5 minutes. Next, the solid phase containing Cr-doped vanadyl hydrogen phosphate sesquihydrate, $VOHPO_4{\cdot}1.5H_2O$ was recovered in an evaporating dish and left to dry in an oven at 85℃ for at least 24 hours. The doped precursor was then pounded into powder form. The precursor synthesis process was repeated with 0.3 mol % (0.0606 g) and 0.5 mol % (0.1010 g) of $Cr(NO_3)_3{\cdot}\ 9H_2O$.

3.2.3 Calcination of Cr-doped and Undoped VPO Catalysts

All precursor powders were prepared in several porcelain boats (Figure 3.3) and calcined in a tubular furnace with a flow mixture of 0.75 % *n*-butane in air for 24 hours at 460℃.

The calcined catalysts (Figure 3.4) were then denoted as BulkVPO, 0.1CrVPO, 0.3CrVPO and 0.5CrVPO, where 0.1, 0.3 and 0.5 are denoted as 0.1 %, 0.3 % and 0.5 % of chromium-doped VPO catalyst respectively.

Figure 3.3: Pre-calcined $VOHPO_4 \cdot 1.5H_2O$ sample.

Figure 3.4: Calcined VPO catalysts at 460℃ for 24 hours.

3.3 Characterisation Techniques and Instrumentation

There were several characterisation methods used to study the promoted VPO catalyst in this experimental study for both physical and chemical analyses. To determine the physical characteristics, the X-ray Diffractometer (XRD), BET surface area measurement and Scanning Electron Microscope (SEM) were used. As for chemical properties, the catalysts were analysed with EDX (Energy-Dispersive X-ray Spectroscopy) Redox Titration and Inductively Coupled Plasma – Optical Emission Spectroscopy (ICP-OES).

3.3.1 X-ray Diffraction (XRD) Analysis

X-ray Diffraction (XRD) is an analytical technique used to characterize the crystallographic structure, crystallite size and preferred orientation in polycrystalline or powdered solid samples. It is notably used for catalysts characterization to identify the crystalline phases in a lattice structure and to obtain an indication of particle size in terms of unit cell dimensions. (Chorkendorff and Niemantsverdriet, 2003)

X-ray diffraction is based on constructive interference of scattered monochromatic X-rays upon diffraction by the crystalline phases. There are ample possible diffraction directions of the lattice which can be obtained from the random orientation of the powdered material. The sample is scanned through a range of 2θ-angles and is measured with diffractograms. The diffractional patterns from the diffractrograms are used to identify the crystallographic phases present in the catalyst. (Chorkendorff and Niemantsverdriet, 2003)

From the angle of maximum intensity, the lattice spacing can then be determined by Bragg's equation (Chorkendorff and Niemantsverdriet, 2003):

$$n\lambda = 2d\sin\theta \tag{3.1}$$

where

n = order of reflection

d = lattice spacing

λ = wavelength

θ = diffraction angle

Each element has its own unique lattice arrangement which is the prominent property determined in XRD. XRD analysis is carried out to determine the composition or relative abundance of V^{4+} and V^{5+} phases. The crystallite size, L can be determined with Scherrer relation (Chorkendorff and Niemantsverdriet, 2003):

$$\langle L \rangle = \frac{\kappa\lambda}{\beta\cos\theta} \tag{3.2}$$

where, β is the peak width, κ is a constant usually taken as 1.

In this experimental study, the XRD patterns were obtained using Shimadzu XRD-6000 diffractometer model (Figure 3.2) employing CuKα radiation generated by Philips glass diffraction X-ray tube broad focus 2.7 kW type on the Cr-doped VPO catalysts at ambient temperature, with basal spacing determined with powder diffraction technique. The catalysts were scanned at a range of $2\theta = 2°-60°$ with a scanning rate of 1.2℃ min^{-1}. The diffractograms obtained were matched with the Joint Committee on Powder Diffraction Standards (JCPDS) PDF 1 database version 2.6 to confirm the catalysts phases.

Figure 3.5 : Shimadzu XRD-6000 diffractometer

3.3.2 BET Multi-Point Surface Area Measurements

BET (Brunauer, Emmett and Teller) multipoint method is a quantitative measurement of specific surface area of a solid, in this case the catalyst by physical adsorption of gas molecules on the catalyst surface. The monolayer capacity of a solid is defined as the amount of adsorbate needed to completely fill a molecular layer on the surface of one gram of solid. The surface area measurement probe normally involves liquid nitrogen with its adsorption isotherm being measured at 77.4 K, its boiling point (Lowell *et al.*, 2004).

A few assumptions have been made in BET's theory involving the Langmuir isotherm. To describe a monolayer adsorption, Langmuir (1916) states that all adsorption sites are energetically equivalent, the surface of the adsorbent is flat, there is no mutual interaction between the adsorbed molecules or atoms (no lateral interactions) and the adsorbed molecules or atoms are localized (immobile adsorption) (Moulijn *et al.*, 1993).

Technically, adsorption takes place mainly due to the weak intermolecular forces of attraction between the gas molecule and the solid surface, usually with van der Waals forces and is reversible. Layers and layers of gas molecules will fill up the active site of the catalyst. The surface area of each layer can be measured as the amount of gas adsorbed is based on the number of saturated monolayer formed. The monolayer capacity is defined as the amount of adsorbed gas molecules able to be accommodated in a completely filled single layer of molecule on the surface of one gram of solid (cm^2/g). N_2 is commonly used to partake in the measurement of a solid's adsorption isotherm.

In this experiment, BET surface area measurement was carried out using nitrogen adsorption–desorption at 77 K with ThermoFinnigan Sorptomatic 1990. Initially, catalyst samples would undergo pre-treatment steps to remove impurities and contaminants by introducing a vacuum environment. The initial sample weight was taken before undergoing a blank test, where helium gas was flown through the tube to obtain a blank data for error tolerance purpose. The reactor was then immersed into liquid nitrogen. After that, pure N_2 gas was injected to analyse the adsorption-desorption process of N_2 gas molecules filling the pores of the catalyst sample. The mass of the catalyst after analysis was recorded and the final sample mass was calculated. The number of molecules required to cover the adsorbent surface with monolayer of adsorbed molecules could be estimated, and the surface area was calculated.

Figure 3.6: ThermoFinnigan Sorptomatic 1990 for BET Surface Area Measurement

3.3.3 Redox Titration

The acidic sites of the VPO catalysts are measured using potentiometric titration method, otherwise knowns as the Niwa and Murakami method. The redox titration is carried out to obtain the average valence (*AV*) of VPO catalyst to determine the average oxidation state of vanadium phase present in the bulk and doped catalyst. Titration is generally carried out with a glass electrode readily calibrated with standard buffer solutions. The acid strength and the average oxidation state of vanadium in the sample can be determined from the acidity value measured by the pH probe.

In this experimental study, a known amount of VPO catalyst was dissolved in 100 ml sulphuric acid, H_2SO_4 2 M. The solution was firstly titrated with potassium permanganate, $KMnO_4$ 0.01 N to oxidize V^{3+} and V^{4+} phases to V^{5+} phase. The change of colour was determined with diphenylamine. End point was reached when the colour of the solution changed from greenish blue to pink. The volume of $KMnO_4$ used was recorded as V1. Next, the solution was treated with ammonium iron(II)sulphate solution at 0.01 N to reduce V^{5+} to V^{4+}. The end point was reached when diphenylamine, the indicator, changed from purple to colourless. The volume of ammonium iron(II)sulphate solution used was recorded as V2.

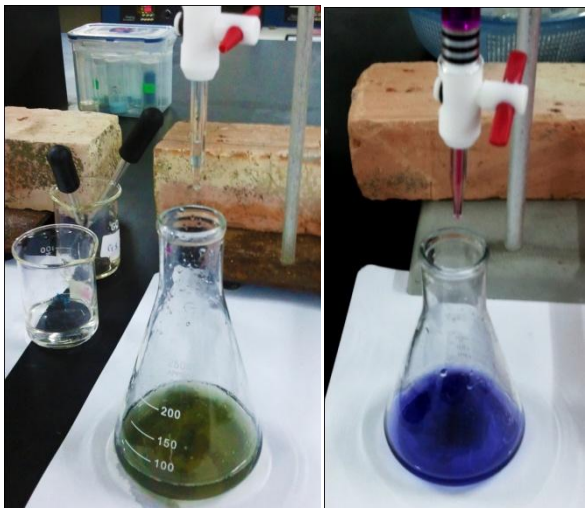

Figure 3.7 : Niwa and Murakami redox titration method apparatus setup.

On a separate account, 25 ml of the original solution was titrated with ammonium iron (II) sulphate solution 0.01 N with diphenylamine as the indicator. This was to determine the amount of V5+ phase present in the original solution. The end point was reached when the solution changed from purple to greenish blue. The volume of ammonium iron (II) sulphate solution used was labelled V3.

The average oxidation state can be determined with the equation below:

$$\mathrm{V}_{AV} = \frac{5\mathrm{V}^{5+} + 4\mathrm{V}^{4+}}{\mathrm{V}^{5+} + \mathrm{V}^{4+}} \qquad (3.3)$$

where

$V^{4+} = 40(0.01)[\mathrm{V2} - \mathrm{V3}] - 20(0.01)[\mathrm{V1}]$

$V^{5+} = 20(0.01)[\mathrm{V3}]$

V_{AV} = the average valence of VPO

3.3.4 Inductively Coupled Plasma – Optical Emission Spectrometry (ICP-OES)

Iductively Coupled Plasma – Optical Emission Spectroscopy (ICP-OES) is a qualitative measurement in which a plasma flame is used to ionize the analyte into vapour phase. When the excited atom or ion returns to ground state, a line spectrum is emitted. The measurement of the line spectrum intensity is then measured by a detector, normally the charged couple device (CCD). The emission intensity depends on the concentration of ionized atoms present in the vapour phase and relies critically on the plasma temperature (Skoog, West, Holler, and Crouch, 2004).

The flame in OES serves a dual purpose, both as an excitation source as well as an emission source. ICP is a high energy source that can excite most elements, be it metallic or non- metallic compounds to produce continuous line-rich spectra. Commercial ICP uses argon as the plasma source. The temperature of plasma ranges from 6500 K to 10000 K, in which almost any element will be atomized and excited to a certain energy level.

The energy released follows the Planck's energy relation:

$$E = \frac{hc}{\lambda} \tag{3.4}$$

where,
h = the Planck's constant
c = velocity of light and λ is wavelength.

The wavelength energy released is said to be unique with individual excited element. The intensity of energy emitted at a chosen wavelength is proportional to the amount of the ions analysed. As such, by determining the wavelengths and its intensity, the sample can be determined with fingerprint identity matching relative to a reference standard (Skoog *et al.*, 2004).

In this study, Perkin-Elmer Emission Spectrometer Model Plasma 1000 is used. Standard solutions consisting components *i.e*. V, P, Cr and a blank sample were prepared to plot calibration curves for the ICP. The catalyst samples were dissolved in 10 ml of HNO_3 and topped up with de-ionised water in volumetric flasks. Next, the samples were introduced into the chamber to be atomized. The line spectra emitted from the ionized sample were detected and analysed.

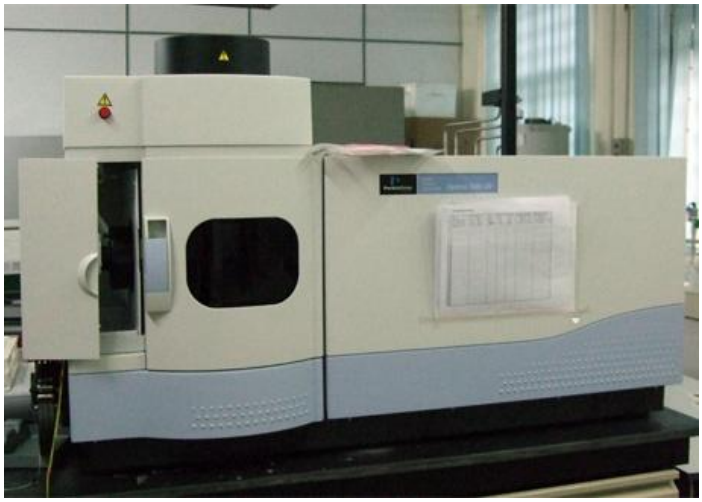

Figure 3.8: Perkin-Elmer Emission Spectrometer Model Plasma 1000

3.3.5 Scanning Electron Microscope (SEM) and Energy-Dispersive X-ray Spectroscopy (EDX)

SEM is an electron microscope which uses a focused beam of high-energy electrons to generate images at the surface of the solid specimens at a very fine scale. SEM analysis is non-destructive because the X-ray generated by electron interactions is mild and does not cause volume loss of the sample. As such, the same sample can be re-used for repetitive analyses.

There are four major components for SEM, namely the electron source, aperture, magnetic lens and bulk specimen interactions. The electron beam is first produced by heating a metallic filament, often a thermionic electron gun. Figure 3.5 illustrates the basic built of an SEM. The electron gun will transmit a narrow high-energy electron beam which will make its way through the aperture and magnetic lenses before reaching the sample. As the electron collides with the sample surface, they will raster and create backscattered electrons, secondary electrons, Auger electrons, and X-ray (Chorkendorff and Niemantsverdriet, 2003).

The detectors will detect the yield of backscattered or secondary electrons and convert them to signals which in turn, produce images. Backscattering becomes more intense with increasing atomic mass. This is because higher mass atoms will produce more backscattered electrons upon collision with the sample surface. As more backscattered electrons are detected, the images will become brighter (Chorkendorff and Niemantsverdriet, 2003).

SEM provides information on the topography, morphology, chemical composition and crystallographic structure of an examined object. The topography shows the general surface feature of an object and its texture to nanometer scale. On the other hand, the morphology shows the shape and size of the particles making up the object on the surface of the sample in nanometer scale as well. The chemical composition tells what elements and compounds the sample comprises, together with its relative abundance. The sample's composition can be detected with energy-dispersive X-ray analysis, EDX. As for crystallographic structure determination, it

provides information on the arrangement of atoms and their degree of lattice order (Chorkendorff and Niemantsverdriet, 2003).

In this experiment, Hitachi S-3400N SEM and EDAX were used to determine the morphological structure and detect the composition of Cr-doped and undoped VPO catalyst samples. Each sample was observed at approximately ×3k to ×16k magnifications using secondary electron, SE bombardment. The SEM micrographs were then selected and print-screened accordingly. The same micrograph was then analysed with EDAX to determine the composition of a particularly focused catalyst sample particle.

Figure 3.9: Hitachi S-3400N SEM and EDAX

CHAPTER 4

RESULTS AND DISCUSSION

4.1 X-ray Diffraction Analysis

From the XRD diffractograms obtained in Figure 4.1 and results of crystallite sizes from Table 4.1, it is found that as the dopant concentration increases, there is an increase in the $VOPO_4$ phase. The crystallite sizes for planes (0 2 0) and (2 2 1) generally do not defer much. The crystalinity is such as well. This shows that the small amount of chromium added does not contribute to the crystallite size of the planes. However, there is a decrement in crystallite size for (2 0 4) plane from 111.31 Å to 95.55 Å. It is initially deduced that the decreasing crystallite size will contribute to having bigger specific surface area for the catalyst powder sizes.

Table 4.1: Crystallite sizes measured on different planes of $(VO)_2P_2O_7$ phase.

Catalysts	Crystallite sizes[d] (Å)			Crystalinity
	Linewidth[a] (0 2 0)	Linewidth[b] (2 0 4)	Linewidth[c] (2 2 1)	
BulkVPO	66.89	111.31	106.64	28.29
0.1CrVPO	69.22	111.34	113.49	27.78
0.3CrVPO	70.62	97.51	91.50	28.04
0.5CrVPO	69.22	95.55	109.11	27.58

[a] FWHM of (020) reflection

[b] FWHM of (204) reflection

[c] FWHM of (221) reflection

[d] Crystallite sizes by means of Scherrer's formula

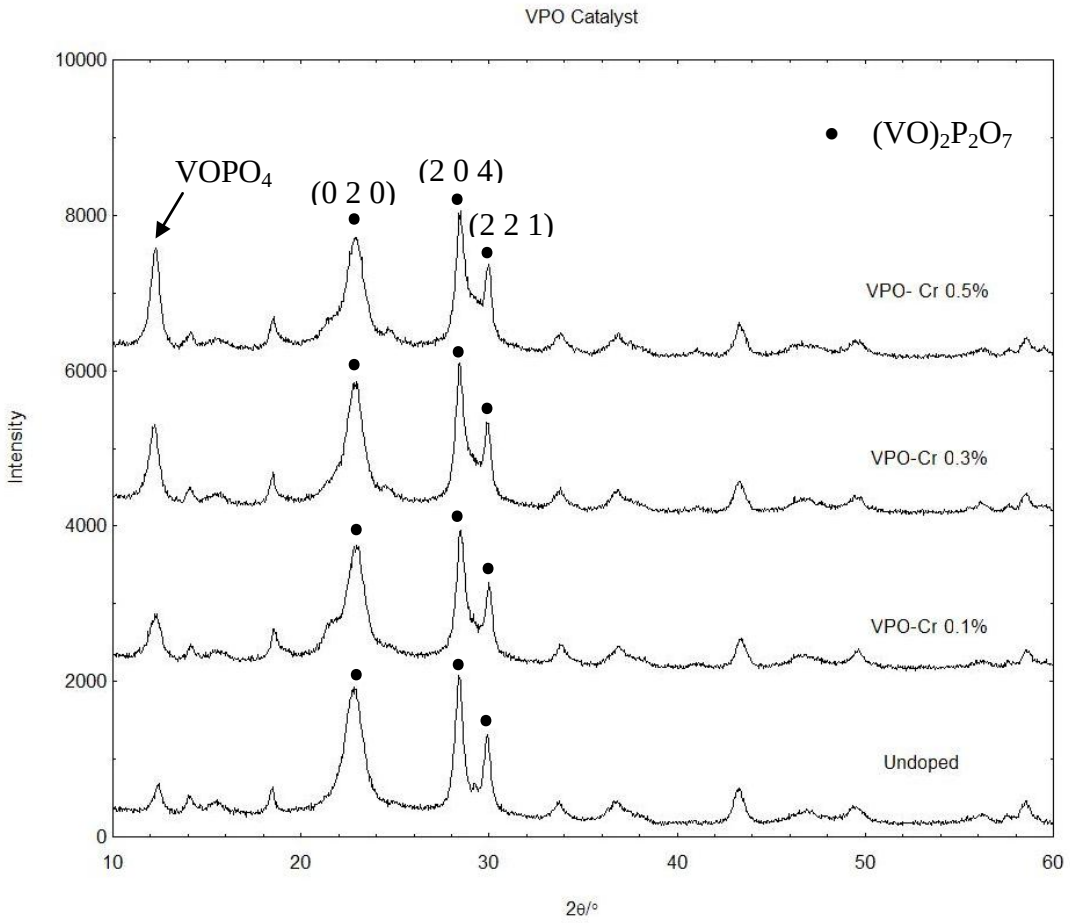

Figure 4.1: XRD diffractograms of various concentration of chromium on VPO catalysts.

4.2 BET Surface Area Analysis

From Table 4.2, it is found that the specific surface area of the catalyst increases from 8.76 $m^2 g^{-1}$ to 27.32 $m^2 g^{-1}$. Initially, the surface area for bulk sample is 8.76 $m^2 g^{-1}$. When 0.1 wt% chromium is added, it becomes 12.11 $m^2 g^{-1}$, at 0.3 wt% chromium-doped, the specific surface area is 21.37 $m^2 g^{-1}$. Lastly, the surface area for 0.5 wt% chromium is 27.32 $m^2 g^{-1}$.

This is because the presence of chromium dopant intercalating within the crystal lattice of VPO will increase the specific surface area of the sample. The higher the surface area, the more reactants (n-butane) is able to come into contact with the catalyst surface and form maleic anhydride.

Taufiq Yap states that the calcination environment of n-butane generally has bigger surface area (Taufiq-Yap and Saw, 2008), which corresponds to the results. The specific surface areas obtained from the BET analysis are supported by the XRD as discussed in previous section. The addition of chromium dopant will decrease the crystallite size, which is correlated to increasing specific surface area.

Table 4.2: Surface area measured for various dopant concentrations in VPO

Catalysts	Surface Area, $m^2 g^{-1}$
BulkVPO	8.76
0.1CrVPO	12.11
0.3CrVPO	21.37
0.5CrVPO	27.32

4.3 SEM-EDAX

4.3.1 Scanning Electron Microscope, SEM

Figure 4.1−4.5 display the SEM images captured on different VPO catalysts powder samples. From the morphological images obtained, it is observed that all samples contain plate-like crystals formed in rosette agglomerates. The rosette shape formation is due to the sesquihydrate precursor synthesis route and the n-butane/air calcination environment used for these chromium-doped VPO catalysts and its bulk sample.

The compositional analysis for each sample is conducted by EDAX and is discussed in subsection 4.3.2.

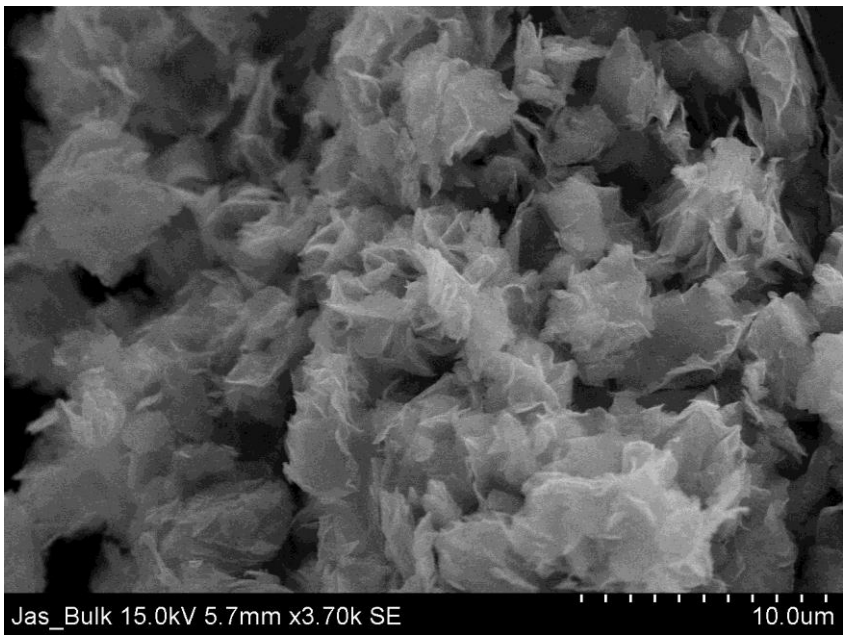

(a)

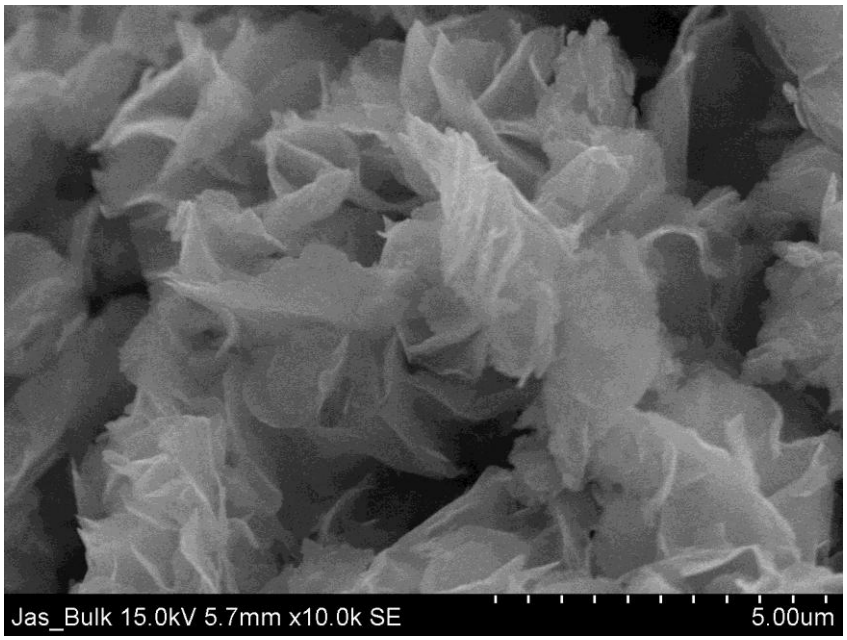

(b)

Figure 4.2: SEM micrograph of BulkVPO at ×3.7k (a) and ×10.0k (b) magnification.

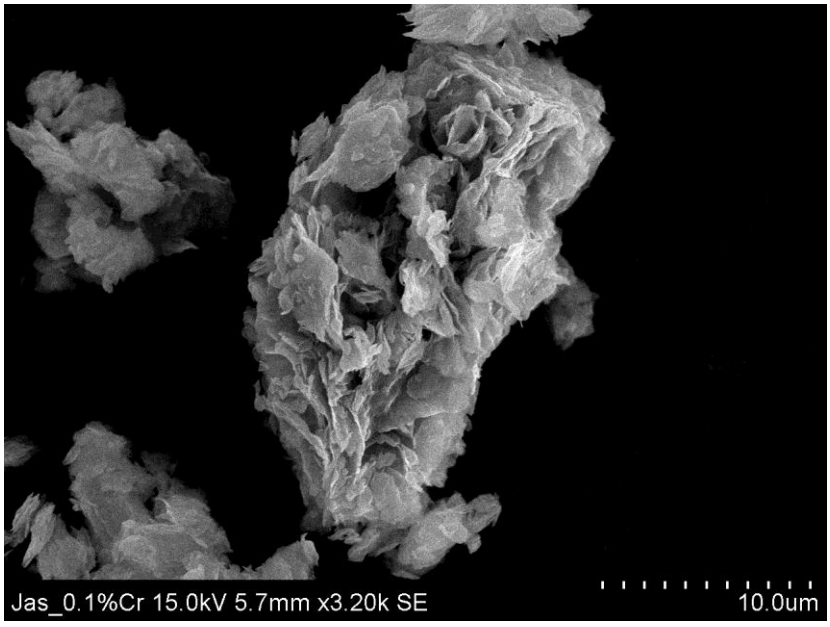

(a)

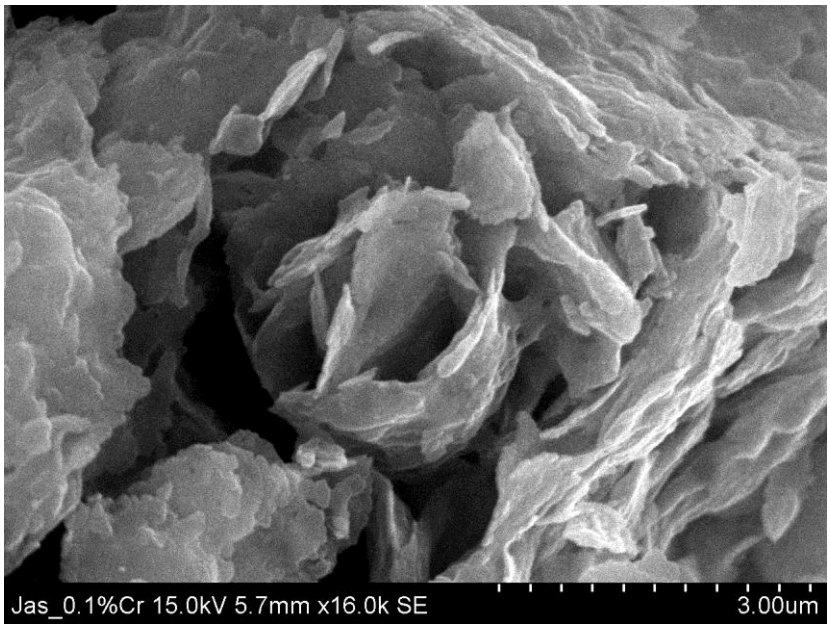

(b)

Figure 4.3: SEM micrograph of 0.1CrVPO at ×3.20k (a) and ×16.0k (b) magnification.

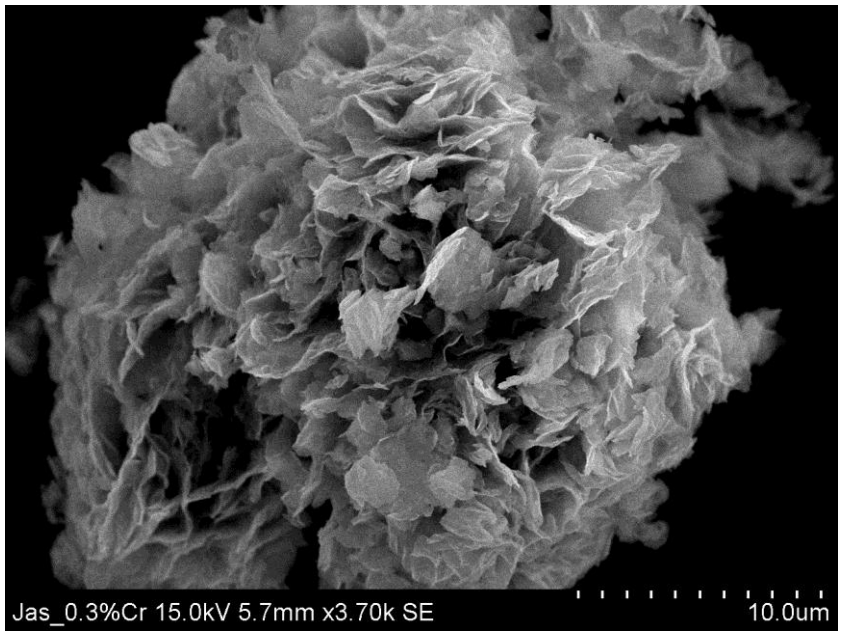

(a)

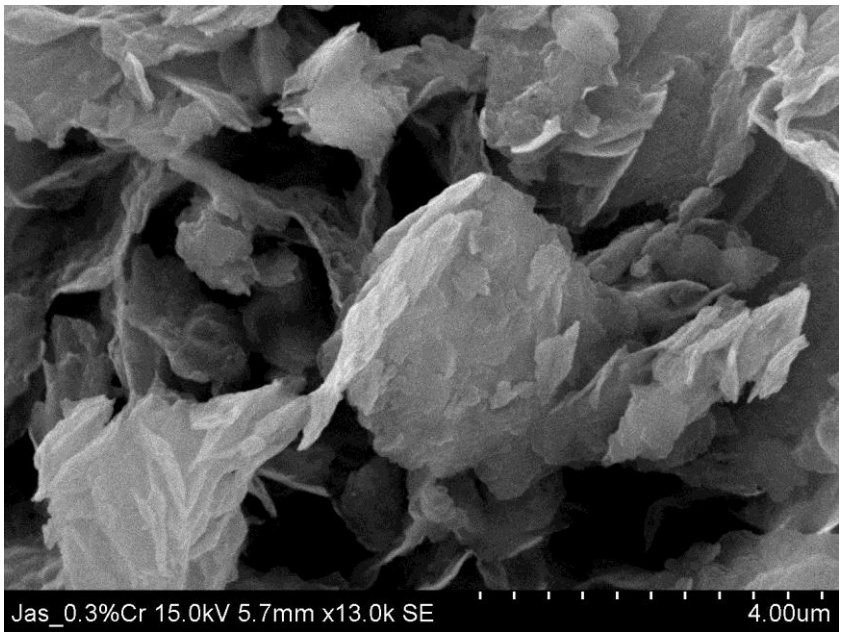

(b)

Figure 4.4: SEM micrograph of 0.3CrVPO at ×3.70k (a) and ×13.0k (b) magnification.

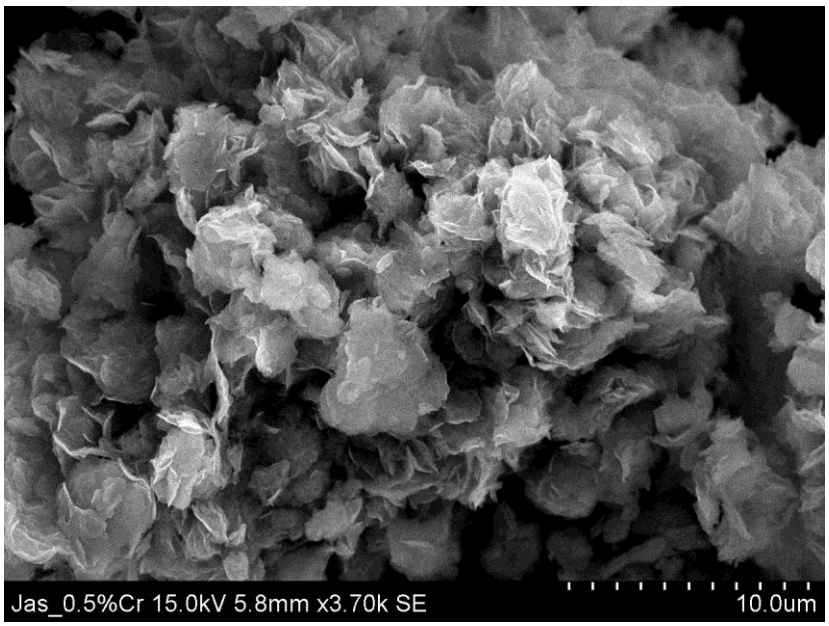

(a)

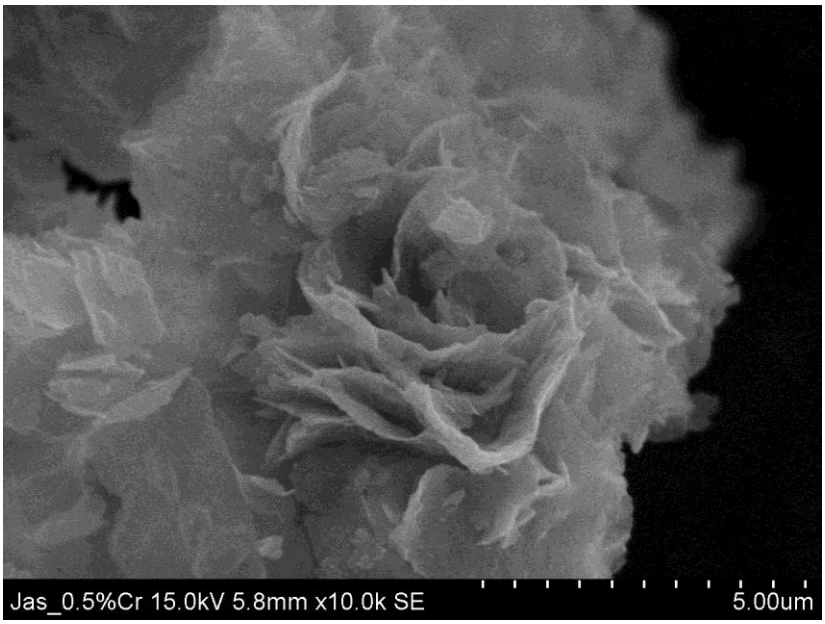

(b)

Figure 4.5: SEM micrograph of 0.5CrVPO at ×3.70k (a) and ×10.0k (b) magnification.

4.3.2 EDAX, Energy-Dispersive X-ray Spectroscopy

EDX analyses were able to confirm the prsence of vanadium, phosphorus and chromium in all catalysts except the bulk sample. The chromium concentration detected at the k-shell increases, with 0.1CrVPO being 0.56 wt%, followed by 0.3CrVPO having 0.66 wt %, and 0.5CrVPO is 1.00 wt %. This has further agreed with the sesquihydrate synthesis route using different dopant concentrations and the bulk catalyst as control sample. However, note that the detection of exact Cr concentration cannot be solely determined by using EDX as the analysis only focuses on one particle instead of the overall sample. Further analysis of catalyst compositions is determined by ICP-OES and will be discussed in section 4.5.

BulkVPO

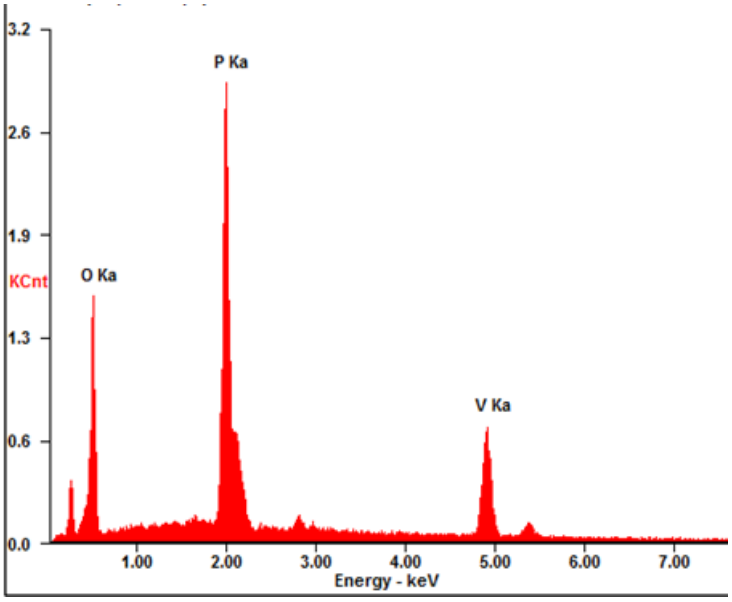

Element	*Wt%*	*At%*
OK	36.88	59.60
PK	25.57	21.35
VK	37.55	19.06

0.1CrVPO

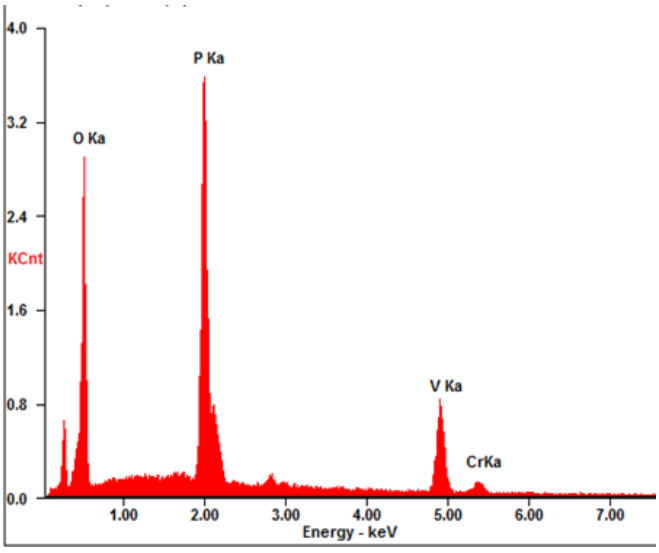

Element	*Wt%*	*At%*
OK	29.24	51.45
PK	26.54	24.12
VK	43.66	24.12
CrK	0.56	0.30

0.3CrVPO

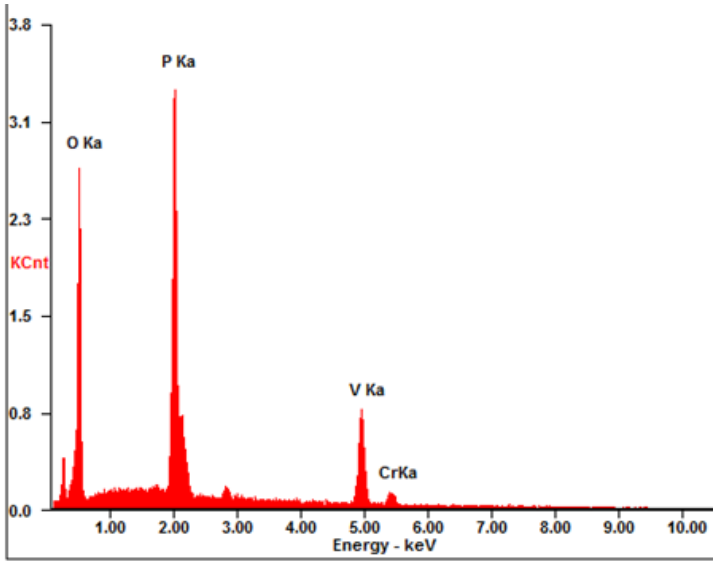

Element	*Wt%*	*At%*
OK	33.10	55.71
PK	26.18	22.76
VK	40.07	21.18
CrK	0.66	0.34

0.5CrVPO

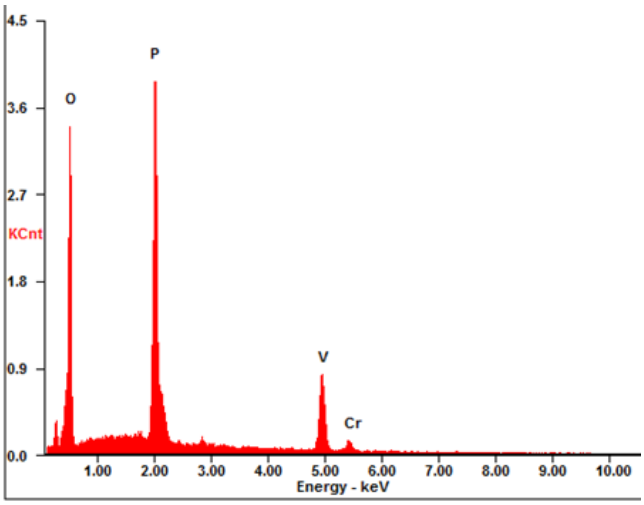

Element	*Wt%*	*At%*
OK	28.21	50.39
PK	25.88	23.87
VK	44.91	25.19
CrK	01.00	00.55

4.4 Redox Titration

From the table above, it is found that the average valence of doped catalyst increases from 4.2326 to 4.7021. The average V^{5+} phase increases with the addition of chromium dopant. Initially, the bulk sample contains 23.26 % V^{5+} phase. With addition of 0.1 wt % chromium, the V^{5+} increases to 45.95 %. At 0.3 wt% chromium, V5+ increases 6.85 % to 52.80 %. At 0.5 wt% chromium, V^{5+} phase increases to 70.21 %. The percentage of V^{4+} phase decreases on the other hand, decreases substantially. The trend is such because the amount of V^{5+} and V^{4+} is inversely proportional to each other.

The increment of average valence number is correlated to the $VOPO_4$ which contains V^{5+} phase detected in the XRD analysis as discussed in prior section. Based on these evaluations, it may be concluded that the selectivity of the catalyst will increase with the increment of varying chromium dopant concentrations.

Table 4.3: Average oxidation numbers of vanadium

Catalysts	Average Valence (V_{AV})	V^{5+} (%)	V^{4+} (%)
BulkVPO	4.23	23.26	76.74
0.1CrVPO	4.45	45.95	54.05
0.3CrVPO	4.52	52.80	47.20
0.5CrVPO	4.70	70.21	29.79

4.5 Inductively Coupled Plasma –Optical Emission Spectroscopy

Based on the ICP-OES results, it is found that the average P/V is 1.28 with the optimum range of P/V being 1.1 to 1.3. The P/V obtained is on the higher side of the range is due to the higher amount of phosphorus being dispersed around the catalyst, which is the way how the catalyst is prepared during precursor synthesis stage. Abon and Volta mentioned that the P/V ratio at the level of the preparation and the activation conditions would strongly influence the final phase composition of the catalysts, particularly the distribution of phosphorus and vanadium and its oxidation state. (Abon and Volta, 1997)

It is agreeable because in the event of calcinations, it is found that most of the synthesized catalyst samples were greenish grey, a sign of oxidized VPO. Taufiq Yap et al. suggested that P/V ratio was one of the key factors in catalyst preparation to avoid the oxidation of $(VO)_2P_2O_7$ and/or of the intermediate amorphous phase to a V^{5+} phosphate. As such, having higher V^{5+} phase present in the VPO catalyst system will have higher selectivity of n-butane to form maleic anhydride. (Taufiq-Yap and Saw, 2008)

Table 4.4: P/V ratio for various doped VPO concentrations from ICP-OES.

Catalysts	P/V	Average P/V
BulkVPO	1.29	1.28
0.1CrVPO	1.35	
0.3CrVPO	1.26	
0.5CrVPO	1.18	

CHAPTER 5

CONCLUSIONS AND RECOMMENDATIONS

5.1 Conclusions

From the analyses, it is found that addition of chromium will increase the selectivity of the VPO catalyst.

Based on the XRD analysis, it is found that as the dopant concentration increases, there is an increase in the $VOPO_4$ phase. Decreasing crystallite size will contribute to having bigger specific surface area for the catalyst powder sizes.

The specific surface areas obtained from the BET analysis are supported by the XRD. The addition of chromium dopant will decrease the crystallite size, correlating to increment of specific surface area.

All n-butane calcined catalyst exhibits plate-like crystals agglomerated into rosette shape. The EDX analysis has also found that there are traces of vanadium, phosphorus and chromium in all catalysts except the bulk sample with increasing amount of chromium.

The average valence number obtained from redox titration increases with increasing chromium concentration. It is believed that the concentration of V^{5+} phase present is inversely proportional to the V^{4+} phase. This means that as the amount of dopant increases, more V^{5+} phase is formed in the VPO catalyst, which corresponds to the selectivity of the VPO catalysts.

The P/V ratio for the VPO catalysts is around 1.28. This is due to higher amount of phosphorus being dispersed around the catalyst and the way the precursor is prepared during synthesis stage.

5.2 Recommendations

There are many challenges experienced by the author throughout the final year project. Among those is the schedule arrangement in using laboratory instruments. The number of final year project students for this batch is higher than previous semesters, with many of them using the same instruments for analysis purposes. As such, all analyses are turn-based. This has indirectly caused a competition among the students wanting to use the same instrument at the same time.

Due to unforeseen circumstances during the experiment, several instruments had malfunctioned or were low on reaction gas. The maintenance and ordering for replacement gas cylinders had taken a long period of time. This had inevitably led to the postponing of schedule as well. Owing to the delay, the catalytic activities of the VPO catalysts were not completed. The analysis was therefore excluded from this thesis.

To curb the problems, it is strongly suggested that limiting the number of final year project student intake per batch will prevent the scenario of having lengthy schedule, frequent breakdown of the instruments which will delay the laboratory work progress. Moreover, it is essential that fellow students take good care of the instruments while conducting analyses. This is to prevent unexpected technical malfunction of the machines which will affect the work progress. Lastly, having a properly arranged schedule and ensuring fellow students adhere to the time while conducting their experiments will greatly aide everyone’s efficiency in the project.

REFERENCES

Abon, M., and Volta, J.-C. (1997). Vanadium phosphorus oxides for n-butane oxidation to maleic anhydride. *Applied Catalysis* , 173-193.

Au, C. T., Chen, X., Wang, Z. Y., Ji, W., and Chen, Y. (2004). The novel and highly selective fumed silica-supported VPO for partial oxidation of n-butane to maleic anhydride. *Catalysis Today* , 223-228.

Baerns, M., and Do, N. T. (1988). Effect of support material on the catalytic performance of V2O5/P2O5 catalysts for the selective oxidation of but-1-ene and furan to maleic anhydride and its consecutive nonselective oxidation. *Applied Catalysis* , 1-7.

Centi, G., and Perathoner, S. (2003). Catalysis and Sustainable (Green) Chemistry. *Catalysis Today* , 287-297.

Chorkendorff, I., and Niemantsverdriet, J. W. (2003). *Concepts of Modern Catalysis and Kinetics.* Germany: Wiley-VCH.

Fogler, H. S. (2006). *Elements of Chemical Reaction Engineering 4th Ed.* USA: Pearson.

Garbassi, F., Bart, J. C., Tassinari, R., Vlaic, G., and Lagarde, P. (1986). Catalytic n-butane oxidation activity and physicochemical characterization of vanadium-phosphorus oxides with variable P/V ratio. *Journal of Catalysis* , 317-325.

Hutchings, G. J. (1990). *Applied Catalysis* , 72.

Hutchings, G. J., Griesel, L., Bartley, J. K., and Wells, R. P. (2003). Preparation of vanadium phosphate catalysts from VOPO4.2H2O: effect of VOPO4.2H2O preparation on catalyst performance. *Journal of Molecular Catalysis* , 113-119.

Ishimura, T., Sugiyama, S., and Hayashi, H. (2000). Vanadyl hydrogenphosphate sesquihydrate as a precursor for preparation of (VO)2P2O7 and cobalt-incorporated catalysts. *Journal of Molecular Catalysis* , 559-565.

Ji, W., Nie, W., Wang, Z., Chen, Y., and Au, C. T. (2003). Comparative studies on the VPO specimen supported on mesoporous Al-containing MCM-41 and large-pore silica. *Applied Catalysis* , 265-272.

Lombardo, E. A., and Pierini, B. T. (2005). Structure and properties of Cr promoted VPO catalysts. *Materials Chemistry and Physics* , 197-204.

Lowell, S., Shields, J. E., Thomas, M. A., and Thommes, M. (2004). *Characterization of Porous Solids and Powders: Surface Area, Pore Size and Density.* Netherlands: Kluwer Academic Publishers.

Moulijn, J. A., van Leeuwen, P. W., and van Santen, R. A. (1993). *Catalysis an integrated approach to homogeneous, heterogeneous and industrial catalysis.* Netherlands: Elsevier.

Oyama, S. T., and Somorjai, G. A. (1986). *Journal of Chemical Education* , 765.

Skoog, D. A., West, D. M., Holler, F. J., and Crouch, S. R. (2004). *Fundamentals of Analytical Chemistry 8th Edition.* Canada: Thomson.

Taufiq-Yap. (2006). Effect of Cr and Co promoters addition on vandium phosphate catalysts for mild oxidation of n-butane. *Science Press* , 144-148.

Taufiq-Yap, and Saw, C. S. (2008). Effect of different calcination environments on vanadium phosphate catalysts for selective oxidation of propane and n-butane. *Catalysis Today* , 285-291.

Taufiq-Yap, Y. H., Goh, C. K., Hutchings, G. J., Dummer, N., and Bartley, J. (2008). Influence of Bi-Fe additive on properties of vanadium phosphate catalyst for n-butane oxidation to maleic anhydride. *Catalysis Today* , 408-412.

Taufiq-Yap, Y. H., Leong, L. K., Hussein, M. Z., Irmawati, R., and Abd Hamid, S. B. (2004). Synthesis and characterisation of vanadyl pyrophosphate catalyst via vanadyl hydrogen phosphate sesquihydrate precursor. *Catalysis Today* , 715-722.

APPENDICES

APPENDIX A: XRD standards, diffractograms and crystallite sizes calculation for catalyst and precursor samples

Standard 3

Phosphate

Rad.: CuKa λ: 1.541838 Filter: d-sp: Diff.

Cut off: Int.: Estimation I/Icor.:

Ref: Bordes, E., Courtine, J. Catal., 57, 236 (1979)

Sys.: Orthorhombic S.G.: $Pmc2_1$ (26)

a: 9.751 b: 7.738 c: 16.568 A: 1.2601 C: 2.1411

α: β: γ: Z: mp:

Ref: Ibid.

Dx: Dm: SS/FOM: F_{25} = 1(0.079, 271)

The solid precursors (N H4 V O3 or V2 O5 and N H4 H2 P O4 were powdered and mixed in stoichiometric proportions. The calcination of P:V=1:1 mixing yielded (V O)2 P2 O7 under N2 (600 C). C.D. Cell: a=9.751, b=16.568, c=7.738, a/b=0.5885, c/b=0.4570, S.G.=Pm21b(26). Silicon used as an internal stand. PSC: oP?. Mwt: 307.83. Volume[CD]: 1250.11.

2θ	Int	h	k	l
14.103	20	1	0	2
15.684	20	0	1	2
18.523	20	2	0	0
21.783	10	1	1	3
22.981	100	0	2	0
28.452	100	2	0	4
29.955	50	2	2	1
30.768	20	1	1	5
33.760	50	1	0	6
36.915	50	1	2	5
37.489	20	2	0	6
38.099	20	3	2	2
39.688	20	1	3	3
40.948	20	1	1	7
43.447	50	0	0	8
45.804	20	1	2	7
46.983	20	0	4	0
49.540	20	5	1	2
49.945	10	0	2	8
55.930	10	5	1	5
56.340	20	1	0	10
58.940	50	3	1	9
62.223	10	6	2	1
63.793	50	4	4	3
65.920	50	4	3	7

File no: 34-1 JC-(83).

Standard 4

VOPO4

Vanadyl Phosphate

Rad.: FeKa1 λ: 1.93597 Filter: Mono d-sp:

Cut off: Int.: Estimation I/Icor.:

Ref: Bordes et al., Ann. Chim. (Paris), 8, 105 (1973)

Sys.: Orthorhombic S.G.: Pnma (62)

a: 7.78 b: 6.13 c: 6.97 A: 1.2692 C: 1.1370

α: β: γ: Z: 4 mp:

Ref: Ibid.

Dx: 3.235 Dm: 3.230 SS/FOM: F_{25} = 9(0.040, 68)

Formed by heating. α-V O P O4 · H2 O above 150 C. C.D. Cell: a=6.970, b=7.780, c=6.130, a/b=0.8959, c/b=0.7879, S.G.=Pbnm(62). PSC: oP28. To replace 19-1403. Mwt: 161.91. Volume[CD]: 332.41.

2θ	Int	h	k	l
21.540	80	1	0	1
24.295	80	0	1	1
28.298	30	1	1	1
28.818	30	2	0	0
32.300	60	0	0	2
33.082	100	2	0	1
35.444	60	1	0	2
36.783	100	0	2	0
37.990	60	2	1	1
43.020	60	1	2	1
47.363	30	2	2	0
51.978	60	1	2	2
52.932	60	0	1	3
55.095	10	1	1	3
58.116	30	2	0	3
59.157	60	0	3	1
59.626	30	4	0	0
69.371	30	1	0	4
72.450	30	1	1	4
74.024	30	2	3	2
77.948	80	2	1	4
78.251	80	0	3	3
80.059	80	1	3	3
83.128	10	3	3	2
84.188	10	3	0	4

β- VOPO4

*** Basic Data Process ***

Group : VPO
Data : Jas_Bulk_Cat

Strongest 3 peaks

no.	peak no.	2Theta (deg)	d (A)	I/I1	FWHM (deg)	Intensity (Counts)	Integrated Int (Counts)
1	6	22.7876	3.89924	100	1.19690	1035	29186
2	8	28.3859	3.14167	95	0.72600	982	19403
3	9	29.8355	2.99224	51	0.76130	533	12090

Peak Data List

peak no.	2Theta (deg)	d (A)	I/I1	FWHM (deg)	Intensity (Counts)	Integrated Int (Counts)
1	12.3809	7.14341	17	0.68660	172	3013
2	14.1271	6.26412	10	0.69430	100	1688
3	15.4488	5.73105	8	0.95110	80	2014
4	18.4450	4.80630	13	0.63540	138	2309
5	21.1200	4.20320	9	0.76000	96	3799
6	22.7876	3.89924	100	1.19690	1035	29186
7	24.8400	3.58152	8	2.48000	83	9755
8	28.3859	3.14167	95	0.72600	982	19403
9	29.8355	2.99224	51	0.76130	533	12090
10	33.6874	2.65839	11	0.74950	113	2256
11	36.8622	2.43639	15	1.26220	152	3922
12	37.8000	2.37808	6	1.10000	61	1751
13	43.2461	2.09037	26	0.76500	269	5656
14	46.8040	1.93942	10	1.67200	104	5036
15	49.4320	1.84229	13	1.10400	135	4291
16	56.0600	1.63917	6	1.00000	65	1918
17	57.6400	1.59794	5	0.75200	52	932
18	58.4950	1.57660	15	0.77000	153	2982

θ	FWHM (rad)	T(Å)
11.3938	0.0209	66.8973
14.1930	0.0127	111.3192
14.9178	0.0133	106.6469

Crystallinity

28.2948.

*** Basic Data Process ***

Group : VPO
Data : Jas_1%Cr_Cat

Strongest 3 peaks

no.	peak no.	2Theta (deg)	d (A)	I/I1	FWHM (deg)	Intensity (Counts)	Integrated Int (Counts)
1	12	28.4937	3.13003	100	0.72900	983	21550
2	8	22.8751	3.88452	98	1.15820	959	25149
3	13	29.9200	2.98399	55	0.71380	544	11910

Peak Data List

peak no.	2Theta (deg)	d (A)	I/I1	FWHM (deg)	Intensity (Counts)	Integrated Int (Counts)
1	11.2800	7.83800	3	0.37340	29	428
2	12.2436	7.22321	34	0.77200	336	6860
3	14.1670	6.24657	9	0.58020	84	1211
4	15.5933	5.67826	7	1.05330	67	1848
5	18.6058	4.76512	21	0.67090	210	3313
6	19.3600	4.58116	7	0.80000	67	1801
7	21.7200	4.08843	33	1.23340	328	11124
8	22.8751	3.88452	98	1.15820	959	25149
9	24.7600	3.59291	11	1.02000	105	4250
10	25.5200	3.48761	5	0.00000	52	0
11	27.0400	3.29491	5	0.00000	51	0
12	28.4937	3.13003	100	0.72900	983	21550
13	29.9200	2.98399	55	0.71380	544	11910
14	31.2400	2.86085	4	0.46000	35	1025
15	33.8165	2.64854	14	0.72400	138	3097
16	36.9400	2.43144	15	1.11200	152	3707
17	37.9200	2.37083	6	1.12000	61	1809
18	41.0267	2.19818	3	0.64000	29	483
19	43.3589	2.08520	23	0.70950	224	4430
20	46.4800	1.95219	10	1.12000	96	3070
21	47.7200	1.90431	5	1.04000	53	1773
22	49.5375	1.83861	13	0.83500	128	3190
23	56.1013	1.63806	5	1.05070	52	1560
24	57.6800	1.59692	4	0.77340	43	827
25	58.5790	1.57454	14	0.70200	138	2263
26	59.5600	1.55093	4	0.66660	38	817

$T\,(\text{Å}) = \frac{0.89\lambda}{\text{FWHM (rad)} \times \cos\theta}$

2θ	θ	FWHM (°)	FWHM (rad)	$\lambda = 1.54$ Å
28.4937	14.2469	0.72900	0.0127	111.3458
22.8751	11.4376	1.15820	0.0202	69.2762
29.9200	14.9600	0.71380	0.0125	113.4948

Crystalinity
27.784

*** Basic Data Process ***

Group : VPO
Data : Jas_3%Cat

Strongest 3 peaks

no.	peak no.	2Theta (deg)	d (A)	I/I1	FWHM (deg)	Intensity (Counts)	Integrated Int (Counts)
1	11	28.4688	3.13271	100	0.83110	1003	20551
2	8	22.8381	3.89073	100	1.13340	1001	27645
3	12	29.8000	2.99573	57	0.88820	574	13761

Peak Data List

peak no.	2Theta (deg)	d (A)	I/I1	FWHM (deg)	Intensity (Counts)	Integrated Int (Counts)
1	12.1671	7.26845	54	0.76030	541	11513
2	14.1176	6.26832	8	0.53130	81	1097
3	15.5188	5.70536	7	0.97370	69	1654
4	18.5046	4.79095	17	0.68420	170	3322
5	19.4000	4.57180	4	0.00000	38	0
6	20.4000	4.34989	5	0.86000	49	1389
7	21.2800	4.17196	16	0.89340	157	5067
8	22.8381	3.89073	100	1.13340	1001	27645
9	24.4400	3.63922	14	1.24800	137	6380
10	27.1600	3.28062	6	1.04000	57	2861
11	28.4688	3.13271	100	0.83110	1003	20551
12	29.8000	2.99573	57	0.88820	574	13761
13	31.1600	2.86801	4	0.96000	41	1778
14	33.7200	2.65589	13	0.80000	128	2991
15	36.9700	2.42954	14	1.30000	144	4035
16	38.0000	2.36602	5	0.69340	48	998
17	41.0160	2.19873	3	0.60800	30	461
18	43.2752	2.08904	23	0.76520	229	4641
19	46.8400	1.93802	11	1.81340	106	4288
20	47.6800	1.90582	5	0.00000	52	0
21	49.4425	1.84192	12	0.95500	122	4499
22	56.0952	1.63822	7	0.88380	66	1613
23	57.5200	1.60098	4	0.54660	43	685
24	58.5120	1.57618	14	0.69160	136	2218
25	59.4000	1.55472	5	0.74660	49	1041

$T(\text{Å}) = \frac{0.89\lambda}{\text{FWHM(rad)} \times \cos\theta}$, $\lambda = 1.54$ Å

2θ	θ	FWHM (rad)	T (Å)
23.4688	14.2344	0.0145	97.5182
22.8381	11.4191	0.0198	70.6201
29.8000	14.9000	0.0155	91.5025

Crystalinity 28.0378

*** Basic Data Process ***

Group : VPO
Data : Jas_5%Cr_Cat

Strongest 3 peaks

no.	peak no.	2Theta (deg)	d (A)	I/I1	FWHM (deg)	Intensity (Counts)	Integrated Int (Counts)
1	13	28.5086	3.12843	100	0.84600	1008	22131
2	8	22.8600	3.88706	91	1.16000	919	27047
3	1	12.2384	7.22626	71	0.68920	713	13533
4	14	29.8800	2.98789	60	0.74280	602	13389

Peak Data List

peak no.	2Theta (deg)	d (A)	I/I1	FWHM (deg)	Intensity (Counts)	Integrated Int (Counts)
1	12.2384	7.22626	71	0.68920	713	13533
2	14.1148	6.26955	8	0.58170	84	1215
3	15.5678	5.68751	6	0.96430	64	1581
4	18.5464	4.78025	19	0.67600	187	3063
5	19.3600	4.58116	5	0.64000	46	879
6	20.4400	4.34147	6	0.88000	57	1364
7	21.3200	4.16422	20	0.78660	201	5073
8	22.8600	3.88706	91	1.16000	919	27047
9	24.5600	3.62171	13	1.08000	132	4485
10	25.6000	3.47689	4	0.60000	39	694
11	26.5200	3.35833	3	0.72000	31	506
12	27.2000	3.27589	6	0.82000	61	1926
13	28.5086	3.12843	100	0.84600	1008	22131
14	29.8800	2.98789	60	0.74280	602	13389
15	31.2000	2.86442	4	0.77340	41	1593
16	33.7681	2.65222	14	0.80160	138	3295
17	37.0085	2.42710	15	1.42290	152	4754
18	38.1600	2.35646	5	0.65340	51	1025
19	40.9933	2.19990	4	0.62670	37	648
20	43.3074	2.08756	24	0.74130	238	4831
21	46.8450	1.93782	9	2.11000	91	5262
22	49.5135	1.83945	12	1.08710	124	3795
23	56.1333	1.63720	6	0.86670	61	1640
24	57.6400	1.59794	5	0.66660	50	862
25	58.5417	1.57545	14	0.73260	138	2384
26	59.5200	1.55187	6	0.68000	58	1121

θ	FWHM (rad)	T(Å)
14.2543	0.0148	95.5499
11.4300	0.0202	69.2244
(6.1192	0.0120	114.8712)
14.9400	0.0130	109.1194

Crystalinity
27.5824

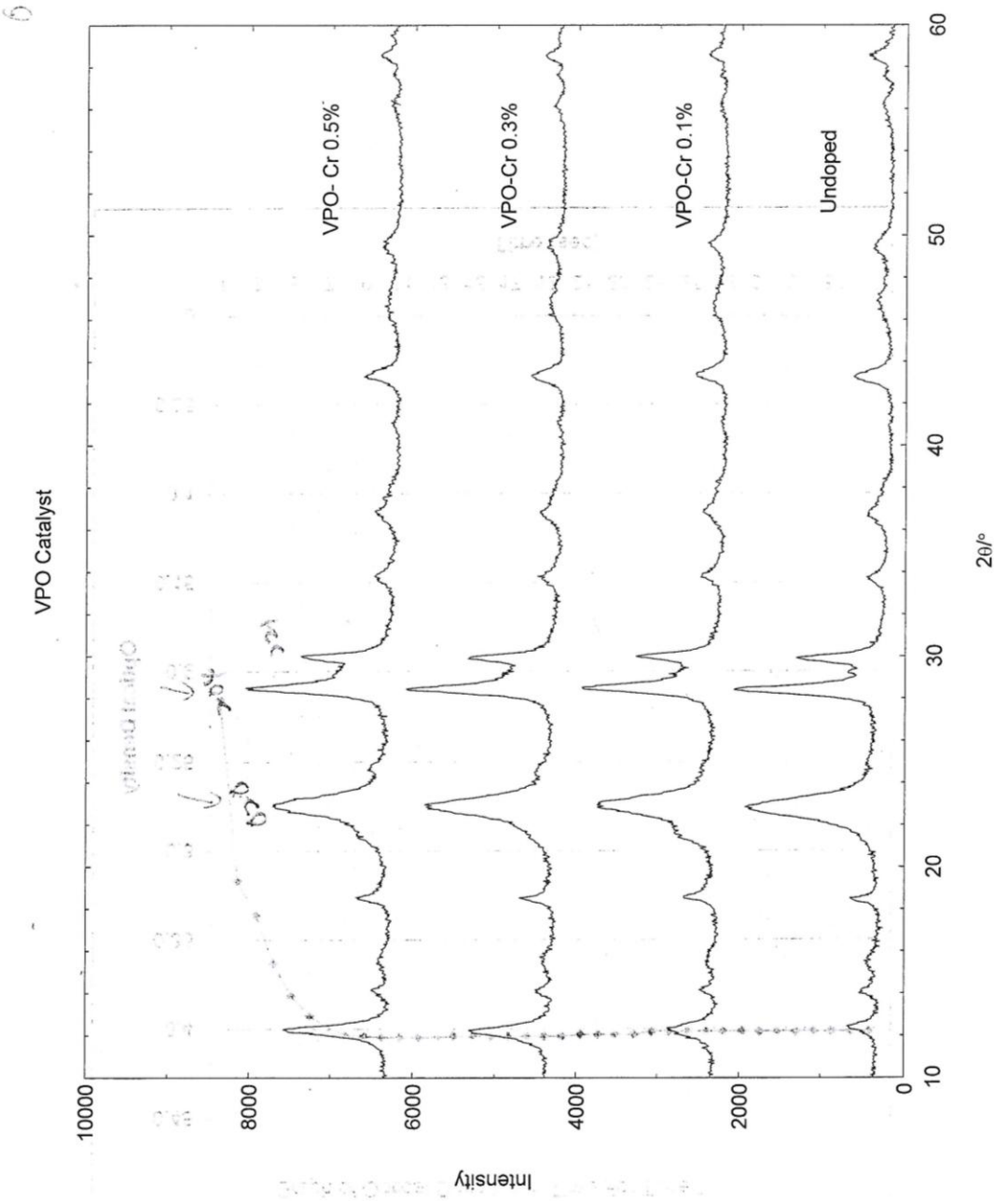
VPO Catalyst
VPO- Cr 0.5%
VPO-Cr 0.3%
VPO-Cr 0.1%
Undoped
Intensity
2θ/°
10000
8000
6000
4000
2000
0
10
20
30
40
50
60

Given the crystallite size formula,

$$T(\text{Å}) = \frac{0.89\lambda}{\text{FWHM(rad)} \times \cos\theta}$$

Where,

λ = 1.54 Å

$$\text{FWHM(rad)} = \text{FWHM(°)} \times \frac{\pi}{180°}$$

	2θ (°)	θ (°)	FWHM (°)	FWHM (rad)	θ (rad)	T (Å)
BulkVPO	22.7876	11.3938	1.1969	0.0209	0.1989	66.9040
	28.3859	14.1930	0.7260	0.0127	0.2478	111.5311
	29.8355	14.9178	0.7613	0.0133	0.2605	106.7099
0.1CrVPO	22.8751	11.4376	1.1582	0.0202	0.1997	69.1502
	28.4937	14.2469	0.7290	0.0127	0.2488	111.0987
	29.9200	14.9600	0.7138	0.0125	0.2612	113.8333
0.3CrVPO	22.8381	11.4191	1.3340	0.0233	0.1994	60.0334
	28.4688	14.2344	0.8311	0.0145	0.2485	97.4449
	29.8000	14.9000	0.8882	0.0155	0.2602	91.4563
0.5CrVPO	22.8600	11.4300	1.1600	0.0203	0.1996	69.0410
	28.5086	14.2543	0.8460	0.0148	0.2489	95.7371
	29.8800	14.9400	0.7248	0.0127	0.2609	112.0952

APPENDIX B: Redox titration preparation, calculation and worksheet

Preparation of diphenylamine, Ph_2NH Indicator

1 g of diphenylamine was weighed and dissolved in a few ml of concentrated sulphuric acid, H_2SO_4. The solution was then transferred into a 100 ml volumetric flask and further topped up with concentrated H_2SO_4.

Preparation of 2 M Sulphuric Acid, H_2SO_4 Solution

Concentrated H_2SO_4 (95−98%)

1L = 1.84 kg = 1840 g/1000 cm^3 = 1.84 g/cm^3

$$\text{Molecular weight of } H_2SO_4 = 2\left(1.00\frac{g}{mol}\right) + 32.07\frac{g}{mol} + 4\left(16.00\frac{g}{mol}\right)$$

$$= 98.07\frac{g}{mol}$$

$$\text{Concentration of } H_2SO_4\ (95-98\%) = \frac{1.84\ g/cm^3}{98.07\ g/mol} \times \frac{95}{100} \times 1000 = 17.82\ M$$

$M_1V_1 = M_2V_2$, where

M_1 = concentration of 95−98% of H_2SO_4

M_2 = concentration of diluted H_2SO_4 (2 M)

V_1 = volume of 95−98% of H_2SO_4

V_2 = volume of diluted H_2SO_4 (2 M)

(17.82 M)(V_1) = (2 M) (1000 cm^3)

∴ V_1 = 112.23 cm^3

Preparation of 0.1 M Sulphuric Acid, H_2SO_4 Solution

$M_1V_1 = M_2V_2$, where

M_1 = concentration of 95−98% of H_2SO_4

M_2 = concentration of diluted H_2SO_4 (2 M)

V_1 = volume of 95−98% of H_2SO_4

V_2 = volume of diluted H_2SO_4 (2 M)

(17.82 M)(V_1) = (0.1 M) (1000 cm^3)

∴ V_1 = 5.61 cm^3

Preparation of 0.01 N Potassium Permanganate, $KMnO_4$

Normality, N (eq/L) = M (mol/L) × *n* (eq/mol)

$$MnO^{4-} + 8H^+ + 5e^- \rightleftharpoons Mn^{2+} + 4H_2O$$

$$\text{Molarity} = \frac{\text{N (eq/L)}}{n\ \text{(eq/mol)}} = \frac{0.01}{5} = 0.002\ \text{M}$$

Molecular weight for $KMnO_4$

= 39.10 g/mol + 54.94 g/mol + 4 (16.00 g/mol) = 158.04 g/mol

Weight for $KMnO_4$ in 1000 cm^3 diluted (0.1 M) H_2SO_4

= 0.002 × 158.04 = 0.3161 g

Preparation of 0.01 N Ammonium Iron(II)Sulphate, $(NH_4)_2Fe(SO_4)_2{\cdot}6H_2O$

Normality, N (eq/L) = M (mol/L) × *n* (eq/mol)

$$Fe^{2+} + e^{-} \rightleftharpoons Fe^{3+}$$

$$\text{Molarity} = \frac{\text{N (eq/L)}}{n\ (\text{eq/mol})} = \frac{0.01}{1} = 0.01\ \text{M}$$

Molecular weight for $(NH_4)_2Fe(SO_4)_2{\cdot}6H_2O$
= 2(14.00 g/mol) + 20(1.00 g/mol) + 55.85 g/mol + 2(32.07 g/mol) + 14(16.00 g/mol)
= 391.99 g/mol

Weight for $(NH_4)_2Fe(SO_4)_2{\cdot}6H_2O$ in 1000 cm^3 diluted (0.1 M) H_2SO_4
= 0.01 × 391.99 = 3.9199 g

Calculation Average Oxidation Number

Given equation to calculate average oxidation state:

$$V_{AV} = \frac{5V^{5+} + 4V^{4+}}{V^{5+} + V^{4+}}$$

where,
$V^{4+} = 40(0.01)[V2 - V3] - 20(0.01)[V1]$
$V^{5+} = 20(0.01)[V3]$
V_{AV} = the average valence of VPO

BulkVPO

Stage 1	V1		V2	
	1st	2nd	1st	2nd
Final	24.50	28.20	21.60	32.70
Initial	6.50	11.80	10.20	21.60
Volume titrated	18.00	16.40	11.40	11.10
Average volume	17.20		11.25	

Stage 2	V3		
	1st	2nd	3rd
Final	19.40	16.70	16.20
Initial	18.50	15.60	14.30
Volume titrated	0.90	1.10	1.90
Average volume	1.00		

V^{4+}	0.6600
V^{5+}	0.2000
AV	4.2326

V^{5+} phase	0.2326
V^{4+} phase	0.7674

0.1CrVPO

Stage 1	V1		V2	
	1st	2nd	1st	2nd
Final	21.30	30.90	33.20	14.50
Initial	6.60	16.20	21.10	2.90
Volume titrated	14.70	14.70	12.10	11.60
Average volume	14.70		11.85	

Stage 2	V3		
	1st	2nd	3rd
Final	9.80	14.60	19.00
Initial	7.00	12.00	15.90
Volume titrated	2.80	2.60	3.10
Average volume	2.83		

V^{4+}	0.6667
V^{5+}	0.5667
AV	4.4595

V^{5+} phase	0.4595
V^{4+} phase	0.5405

0.3CrVPO

Stage 1	V1		V2	
	1st	2nd	1st	2nd
Final	17.70	30.00	38.00	27.50
Initial	3.00	16.80	26.00	16.00
Volume titrated	14.70	13.20	12.00	11.50
Average volume	13.95		11.75	

Stage 2	V3		
	1st	2nd	3rd
Final	18.80	35.50	26.00
Initial	15.50	32.20	22.40
Volume titrated	3.30	3.30	3.60
Average volume	3.30		

V^{4+}	0.5900
V^{5+}	0.6600
AV	4.5280

V^{5+} phase	0.5280
V^{4+} phase	0.4720

0.5CrVPO

Stage 1	V1		V2	
	1st	2nd	1st	2nd
Final	32.60	42.00	33.70	44.90
Initial	18.40	27.40	22.50	33.70
Volume titrated	14.20	14.60	11.20	11.20
Average volume	14.40		11.20	

Stage 2	V3		
	1st	2nd	3rd
Final	27.80	32.90	36.20
Initial	25.00	29.60	32.90
Volume titrated	2.80	3.30	3.30
Average volume	3.30		

V^{4+}	0.2800
V^{5+}	0.6600
AV	4.7021

V^{5+} phase	0.7021
V^{4+} phase	0.2979

APPENDIX C: ICP-OES preparation and worksheet

Stock Solution for P (50 ppm)

Molecular weight of $NH_4H_2PO_4$ = 115.03 g/mol

Molecular weight of P = 30.9738 g/mol

∵ 50 ppm = 50 mg/L = 0.05 g/L

Number of mol of P = 0.05 g/L / 30.9738 g/mol = 1.6145×10^{-3} mol

∴ Mass of $Cr(NO_3)_3 \cdot 9H_2O$ = 1.6145×10^{-3} mol × 115.03 g/mol

= 0.1857 g (in 1000 ml)

Standard Solutions for P

The standard solutions were prepared with serial dilution:

$M_1V_1 = M_2V_2$, where

M_1 = concentration of pre-diluted solution

M_2 = concentration of diluted solution

V_1 = volume of pre-diluted solution

V_2 = volume of diluted solution

Concentration, M (ppm)	Volume, V (ml)
50	Stock solution
30	150
20	100
10	50

Stock Solution for V (50 ppm)

Molecular weight of NH_4VO_3 =116.978 g/mol

Molecular weight of V = 50.94 g/mol

∵ 50 ppm = 50 mg/L = 0.05 g/L

Number of mol of Cr = 0.05 g/L / 50.94 g/mol = 9.8155×10^{-4} mol

∴ Mass of $Cr(NO_3)_3\cdot9H_2O$ = 9.8155×10^{-4} mol × 116.978 g/mol

= 0.1148 g (in 1000 ml)

Standard Solutions for Cr

The standard solutions were prepared with serial dilution:

$M_1V_1 = M_2V_2$, where

M_1 = concentration of pre-diluted solution

M_2 = concentration of diluted solution

V_1 = volume of pre-diluted solution

V_2 = volume of diluted solution

Concentration, M (ppm)	Volume, V (ml)
50	Stock solution
30	150
20	100
10	50

Stock Solution for Cr (50 ppm)

Molecular weight of $Cr(NO_3)_3 \cdot 9H_2O$ = 400.15 g/mol

Molecular weight of Cr = 51.996 g/mol

∵ 50 ppm = 50 mg/L = 0.05 g/L

Number of mol of Cr = 0.05 g/L / 51.996 g/mol = 9.6161×10^{-4} mol

∴ Mass of $Cr(NO_3)_3 \cdot 9H_2O$ = 9.6161×10^{-4} mol × 400.15 g/mol

= 0.3849 g (in 1000 ml)

Standard Solutions for Cr

The standard solutions were prepared with serial dilution:

$M_1V_1 = M_2V_2$, where

M_1 = concentration of pre-diluted solution

M_2 = concentration of diluted solution

V_1 = volume of pre-diluted solution

V_2 = volume of diluted solution

Concentration, M (ppm)	Volume, V (ml)
40	200
20	125
10	125
5	125
2.5	125

Preparation of 8 M HNO_3

$$\text{Molarity of } HNO_3 = \frac{\text{Density of } HNO_3}{\text{Molecular weight of } HNO_3} \times \frac{65}{100} \times 1000$$

$$= \frac{1.409 \text{ g/cm}^3}{63.01 \text{ g/mol}} \times 0.65 \times 1000 = 14.53 \text{ M}$$

$M_1V_1 = M_2V_2$, where

M_1 = concentration of pre-diluted solution

M_2 = concentration of diluted solution

V_1 = volume of pre-diluted solution

V_2 = volume of diluted solution

$$V_1 = \frac{(8 \text{ M})(1000 \text{ ml})}{(14.53 \text{ M})} = 550.60 \text{ ml (in 1000 ml)}$$

Preparation of Blank Solution

10 ml of 8 M HNO_3 was diluted in a 250 ml volumetric flask with de-ionised water.

Sample	P mg/L	P g/L	P mol	V mg/L	V g/L	V mol	Dope mg/L	Dope g/L	Dope mol	P/V	Dope/V
BulkVPO	22.14	0.0221	0.000714816	28.11	0.02811	0.000551809	-	-	-	1.295403981	-
0.1CrVPO	22.73	0.0227	0.000733865	27.64	0.02764	0.000542583	0.235	0.000235	4.5195E-06	1.352539176	0.00832974
0.3CrVPO	21.97	0.0219	0.000709327	28.75	0.02875	0.000564373	0.218	0.000218	4.1926E-06	1.256841939	0.00742883
0.5CrVPO	21.44	0.0214	0.000692216	29.85	0.02985	0.000585966	0.250	0.00025	4.8080E-06	1.181323659	0.00820535

P	30.973	g/mol
V	50.9415	g/mol
Cr	51.996	g/mol

Average	P/V	1.284731926
	Cr/V	0.007987977